University of New Mexico
UNM Digital Repository

Civil Engineering ETDs | Engineering ETDs

Summer 7-11-2018

The Investigation of Silica Removal in Reverse Osmosis Concentrate by Changing Design Parameters

John M. Stomp IV
University of New Mexico - Main Campus

Follow this and additional works at: https://digitalrepository.unm.edu/ce_etds

 Part of the Civil and Environmental Engineering Commons

Recommended Citation
Stomp, John M. IV. "The Investigation of Silica Removal in Reverse Osmosis Concentrate by Changing Design Parameters." (2018).
https://digitalrepository.unm.edu/ce_etds/211

This Thesis is brought to you for free and open access by the Engineering ETDs at UNM Digital Repository. It has been accepted for inclusion in Civil Engineering ETDs by an authorized administrator of UNM Digital Repository. For more information, please contact disc@unm.edu.

John M. Stomp IV

Candidate

Civil Engineering

Department

This thesis is approved, and it is acceptable in quality and form for publication:

Approved by the Thesis Committee:

Dr. Kerry Howe, Chairperson

Dr. Bruce Thomson

Dr. José Manuel Cerrato

Dr. Patrick Brady

THE INVESTIGATION OF SILICA REMOVAL IN REVERSE OSMOSIS CONCENTRATE BY CHANGING DESIGN PARAMETERS

by

JOHN STOMP

BACHELOR OF SCIENCE, BIOLOGY

THESIS

Submitted in Partial Fulfillment of the
Requirements for the Degree of

Master of Science
Civil Engineering

The University of New Mexico
Albuquerque, New Mexico

July, 2018

ACKNOWLEDGEMENTS

I would like to acknowledge everyone that has helped me throughout the completion of this work. First, my committee chair Dr. Kerry Howe. Dr. Howe, thank you for accepting me as your graduate student and for all of your expertise, guidance and time given to me throughout my research and in the classroom. Next, I would like to thank my committee members, Dr. Bruce Thomson, Dr. José Cerrato and Dr. Patrick Brady, for all of the knowledge and support you have provided me. Furthermore, thank you to my friends, lab mates and classmates for such a fun and amazing experience. Lastly, I would like to thank all of the teachers, professors, custodians and staff members at the University of New Mexico for working so hard to make my experience enjoyable.

THE INVESTIGATION OF SILICA REMOVAL IN REVERSE OSMOSIS CONCENTRATE BY CHANGING DESIGN PARAMETERS

By

John Stomp

B.S. Biology, University of New Mexico, 2014

M.S. Civil Engineering, University of New Mexico, 2018

ABSTRACT

Silica at high concentrations can precipitate and polymerize, forming scales on heat exchangers, boilers and turbines in industrial equipment, and on the feed side of the semi-permeable membranes in Reverse Osmosis (RO). Silica scale can cause decreased efficiency, increased treatment costs and, in some cases, irreversible damage. The removal of silica scale is challenging because it requires the handling of dangerous and hazardous chemicals. Therefore, much research has gone into the removal of soluble silica. The purpose of this research was to compare the overall effectiveness of silica removal in RO concentrate water with freshly precipitated $Mg(OH)_2$ and $Fe(OH)_3$, and calcined Hydrotalcite (HTC) by changing the design parameters adsorbent dose and pH. To complete this work, 15 experiments (12 batch experiments and 3 flow through experiments) were performed.

Initial batch studies investigated and compared the effects of changing the dose and on silica removal for freshly precipitated $Mg(OH)_2$ and $Fe(OH)_3$, and calcined HTC. The results showed that, for all materials, an increased dose at pH 10 led to increased silica removal. Then, using the three materials, the effect of pH was investigated on silica removal. When the pH was increased from 9 to 11, trends in silica removal varied

for the three materials. Furthermore, batch studies were completed on the three materials to determine the sorption density and sorption kinetics onto the solids. The sorption densities were used to determine the most applicable isotherm (Freundlich or Langmuir) and identify isotherm parameters for the materials. All three materials fit the Freundlich isotherm model and based on isotherm parameters, the largest adsorption capacity was determined to be HTC and the most intense adsorption was determined to be $Fe(OH)_3$. The sorption kinetics were examined for zero, first and second order kinetics to determine a rate constant for silica adsorption reactions. It was discovered that all three materials fit the second order kinetics models and the uptake rates were determined to be 3.0×10^{-4} mg/L·min for $Mg(OH)_2$, 9.0×10^{-5} mg/L·min for $Fe(OH)_3$ and 7.0×10^{-5} mg/L·min for HTC at various doses.

Using the results of the batch tests, a flow through system was constructed and used to examine the material's capacities on a larger scale and determine if 70% silica removal can be maintained. The results showed that when the materials were compared, HTC could achieve the target percent silica removal at a lower dose than $Mg(OH)_2$ and $Fe(OH)_3$ but, all three materials could maintain silica removal on a large scale. This study provides important information for water treatment industries looking to remove soluble silica from water.

Table of Contents

Table of Contents vi

List of Figures ix

List of Tables xi

CHAPTER 1: INTRODUCTION 1

Objective 1 3

Objective 2 3

Objective 3 3

Objective 4 3

Objective 5 3

Objective 6 3

CHAPTER 2: BACKGROUND AND LITERATURE REVIEW 4

Mineral Chemistry of Silica 4

Aqueous Chemistry of Silica 5

Formation of Silica Scale 7

Silica Scale Formation in Cooling Towers and Thermoelectric Power Plants 8

Silica Scale Formation in RO Membranes 8

Prevention of Scale and Fouling 9

Scale Inhibitors 9

pH Adjustments 10

Lime Softening 10

Magnesium Hydroxide 11

Ferric Hydroxide 13

Aluminum Hydroxide 14

Hydrotalcite 16

Discussion on Adsorption vs Surface Precipitation 16

CHAPTER 3: MATERIALS AND METHODS....18

Materials....19

Preparation of Source Water....19

Preparation of Stock Solutions....20

Preparation of Adsorbents....21

Magnesium Hydroxide....21

Ferric Hydroxide....22

Hydrotalcite....23

Analytical Methods....24

Silica Concentration....24

pH....26

Batch Test....27

Objective 1: The Effect of Dose on Silica Removal....27

Objective 2: The Effect of pH on Silica Removal....29

Objective 3: Isotherm Testing....31

Objective 4: Kinetic Testing....33

Objective 5: Silica Removal Mechanism by HTC....34

Flow Through Test....34

Design of Flow Through System....35

Objective 6: Continuous Dosing Flow Through Experiments....38

CHAPTER 4: RESULTS AND DISCUSSION....40

The Effect of Dose on Silica Removal....40

The Effect of pH on Silica Removal....44

Discussion of Silica Removal in Experiments 1 through 6....52

Design Parameters....54

Isotherm Results....55

Adsorption vs. Surface Precipitation Mechanism for Silica Removal....63

Freundlich Isotherm Parameters....63

Kinetic Results....65

Implications of Rate Constants....69
Silica Removal Mechanism by HTC....69
Continuous Membrane Filtration Experiments....72
Experiment 13....74
Experiment 14....75
Experiment 15....76
Membrane Fouling....79
CHAPTER 5: CONCLUSION....81
REFERENCES....87

List of Figures

Figure 1: Log C - pH Diagram of Silicic Acid Between pH Values of 0 And 14 for a Total Dissolved Silica Concentration of 10^{-3} M. 6

Figure 2: Log C - pH Diagram for Insoluble Magnesium Hydroxide. 12

Figure 3: Log C - pH Diagram for Iron(III) Species in Equilibrium with $Fe(OH)_3$ 14

Figure 4: Log C - pH Diagram for Al Species in Equilibrium with $Al(OH)_3$. 15

Figure 5: GE Osmonics RO Unit. 19

Figure 6: DR/890 Colorimeter Reader. 24

Figure 7: Sample Filtration Setup. 25

Figure 8: $Fe(OH)_3$ Filtered by the Pall Corporation Membrane. 25

Figure 9: Results of Hach Test. 26

Figure 10: Centrifuge Used for Experiments. 29

Figure 11: Schematic of the Flow Through System. 35

Figure 12: Little Giant Pump. 36

Figure 13: POREX® membrane. 36

Figure 14: Custom Made Flow Through System. 38

Figure 15: Percent Silica Removal versus Dose at Desired pH 10. 42

Figure 16: Mass Loading (mg/g) on the $Mg(OH)_2$, $Fe(OH)_3$ and HTC at pH 10. 43

Figure 17: Molar Loading (mg/mol) on the $Mg(OH)_2$, $Fe(OH)_3$ and HTC at pH 10. 44

Figure 18: The Percent Silica Removal vs. pH at a 3 mM Dose of $Mg(OH)_2$ 45

Figure 19: The Percent Silica Removal vs. pH at a 3 mM Dose of $Fe(OH)_3$. 46

Figure 20: The Percent Silica Removal vs. pH at a 3 mM Dose of HTC 52

Figure 21: Q_e vs. Final Silica Concentration for $Mg(OH)_2$. 56

Figure 22: Freundlich Isotherm results for $Mg(OH)_2$.....57

Figure 23: Langmuir Isotherm results for $Mg(OH)_2$. 57

Figure 24: Q_e vs. Final Silica Concentration for $Fe(OH)_3$.....59

Figure 25: Freundlich Isotherm results for $Fe(OH)_3$. 59

Figure 26: Langmuir Isotherm results for $Fe(OH)_3$.....60

Figure 27: Q_e vs. Final Silica Concentration for HTC. 61

Figure 28: Freundlich Isotherm results for HTC.....62

Figure 29: Langmuir Isotherm results for HTC. 62

Figure 30: Zero Order Kinetic results.....67

Figure 31: First Order Kinetic results. 68

Figure 32: Second Order Kinetic results. 68

Figure 33: A theoretical CMFR used for the mass balance calculations. 69

Figure 34: Flow Through Experimentation Using New $Mg(OH)_2$ Every Hour. 74

Figure 35: Flow Through Experimentation Using New $Fe(OH)_3$ Doses Every Hour. 76

Figure 36: Flow Through Experimentation with Single Dose of HTC. 77

Figure 37: Flow Through Experimentation Using New HTC Doses Every Hour. 78

Figure 38: The Membrane Flux vs. Time in Experiments 13 Through 15. 80

List of Tables

Table 1: Silica Speciation From pH 7 to pH 14. 7

Table 2: RO Concentrate Water Composition. 20

Table 3: Composition of Stock Solutions. 21

Table 4: Equations Used to Prepare $Mg(OH)_2$ 22

Table 5: Equations Used to Prepare $Fe(OH)_3$. 23

Table 6: Summary of Parameters Used in Experiments 1 Through 3. 28

Table 7: Summary of Parameters Used in Experiments 4 Through 6. 30

Table 8: Summary of Parameters Used in Experiments 7 Through 9. 32

Table 9: Summary of Parameters Used in Experiments 10 Through 12. 33

Table 10: Summary of Desired Parameters Used in Experiments 13 Through 15. 39

Table 11: Summary of pH Results for Experiments 1 Through 3. 41

Table 12: Summary of pH Results for Experiments 4 Through 6. 47

Table 13: The magnesium concentrations calculated at pH values 9, 10 and 11 48

Table 14: The dissolution of the preformed $Mg(OH)_2$ doses in the RO concentrate water. 49

Table 15: The iron(III) concentrations determined at pH values 9, 10 and 11. 50

Table 16: Point of Zero Charge for silica, $Mg(OH)_2$, $Fe(OH)_3$ and HTC. 53

Table 17: The Freundlich Isotherm Parameters. 65

Table 18: The calculations for how many moles of silica were bound to HTC per release of hydroxyl groups. 71

Table 19: The calculations for how many moles of silica were bound to HTC per release of hydroxyl groups in the RO concentrate water. 72

Table 20: A summary of parameters used in each experiment. 73

CHAPTER 1: INTRODUCTION

In the United States, surface and groundwater is an important resource used for drinking water, irrigation, industry and thermoelectric power generation. One constituent found in both surface and groundwater is silica. Silica is found in almost all natural water sources ranging in concentrations from 1 mg/L to 60 mg/L (Ning, 2005). For references purposes, the drinking water in Albuquerque, New Mexico, which is a blend of surface and ground water, has silica concentrations ranging from 30 – 50 mg/L. Silica content becomes problematic for thermoelectric power industries and reverse osmosis (RO) membranes when concentrations of silica in water exceed the solubility limit, forming silica scales.

Silica scales have been observed in heat exchangers, boilers and turbines in industrial equipment and on the feed side of the semi-permeable membranes in RO. In industrial equipment, silica scale can cause disruptions by decreasing the heat transfer efficiency and increased operational cost (Al-Mutaz and Al-Anezi, 2004; Baca, 2017; Batchelor et al., 1991; Cob et al. 2014; Dai et al., 2016; Den and Wang, 2008; Iler, 1974; Sheikholeslami and Bright, 2002). Silica scale in RO can cause fouling, which can lead to lower efficiencies, increased pressure and, in some cases, the membranes need to be replaced (Cobb et al., 2014; Den and Wang, 2008; Ning, 2010). Furthermore, the formation of silica scale in RO can cause permeate shut downs and irreversible damage (Amjad and Zuhl, 2011).

The removal of silica scale is difficult because it requires the handling and use of hazardous chemicals such as hydrofluoric acid (HF) (Den and Wang, 2008). Scale inhibitors have been shown to prevent scale depending on pH, temperature, salt

concentration, etc. of the water. However, the addition of scale inhibitors requires the use of large amounts of chemicals. For instance, Reeves Generating Station which is located in Albuquerque, New Mexico and is owned and operated by Public Service Company of New Mexico (PNM), scale inhibitors are used to keep silica dissolved at concentrations above the solubility limit. Reeves Generating Station uses an open loop system to keep conductivity levels low and must continuously feed fresh scale inhibitors (Baca, 2017).

Many methods have been employed to remove silica from water including lime softening, adsorption, co-precipitation, ion-exchange, coagulation and filtration with varying degrees of success (Al-Mutaz and Al-Anezi, 2004; Sims, 2015; Baca, 2017; Sasan et al., 2017; Zhoug et al., 2016). New and improved practices for successful removal of silica are being studied in both laboratory and industrial settings. Sims (2015), research focused on the adsorbent $Mg(OH)_2$ for the removal of silica. Furthermore, Sims (2015) used $Fe(OH)_3$ as an adsorbent which inspired the work of Baca (2017). Similarly, Baca's (2017) work examined $Fe(OH)_3$ as an adsorbent of silica. Additionally, Sasan et al. (2017) showed that hydrotalcite (HTC) could be used as a material that removes silica.

While the above research was important, there was nothing in the findings to compare $Mg(OH)_2$, $Fe(OH)_3$ and HTC in overall effectiveness of silica removal. The purpose of this paper is to directly compare the three silica removal strategies $Mg(OH)_2$, $Fe(OH)_3$ and HTC. This was accomplished by changing design parameters and examining how these variations might affect the silica removal process. The design parameters examined in this work were adsorbent dose and pH. The major objectives of this research were as follows:

Objective 1: To investigate and compare the doses of the $Mg(OH)_2$, $Fe(OH)_3$ and HTC required to silica removal.

Objective 2: To investigate the effect of pH on silica removal using $Mg(OH)_2$, $Fe(OH)_3$ and HTC.

Objective 3: To investigate and compare the sorption density of silica on $Mg(OH)_2$, $Fe(OH)_3$ and HTC at equilibrium to determine the most applicable adsorption isotherm (Freundlich or Langmuir), and identify isotherm parameters.

Objective 4: To investigate and compare the kinetics of silica sorption onto $Mg(OH)_2$, $Fe(OH)_3$ and HTC.

Objective 5: Due to the limited literature on HTC mechanism, propose a mechanism for how HTC removes silica.

Objective 6: Determining the design parameters (dosing, pH and HRT) for the Flow-Through System.

This research was completed using batch and flow through experiments. Batch testing achieved several objectives. The first purpose was to observe trends in the data when the design parameters are altered. This provided insight into determining the optimal silica design parameters. Next, isotherm and kinetic data was used to assist in the experimental design of a flow through adsorption system. Finally, the batch testing was used to determine the proper dosage and pH for the flow through experiments. The flow through testing provided a unique opportunity to examine the selected design parameters for silica removal in a pilot scale.

CHAPTER 2: BACKGROUND AND LITERATURE REVIEW

The removal of silica to prevent scaling continues to be very important for industrial processes and membrane filtration systems. Removing silica scale is difficult because it requires handling and use of hazardous chemicals and preventing silica scale using scale inhibitors involves large quantities of chemical additions with varying degrees of success. An alternative strategy is to remove dissolved silica to prevent scale formation. This research paper focused on the effectiveness of $Mg(OH)_2$, $Fe(OH)_3$ and HTC in removing silica and examining how variations in the design parameters might affect the silica removal process. Chapter 2 presents a discussion of the chemistry of silica, discussion on the formation of silica scale and a literature review on the methods used to prevent silica scaling and fouling.

Mineral Chemistry of Silica

Silicon is the third most abundant element on Earth, after oxygen and hydrogen (Krivovichev and Charykova, 2012). Silicon has four valence electrons that allow it to bind to oxygen forming the inorganic molecule SiO_2 (called silica). Silica can bind to metals, forming silicates. Silicates are rock-forming minerals that constitute the majority of Earth's crust and mantel (Peslier et al., 2010). Furthermore, silica minerals exist in rocks, soils and sediments due to the variety of bonds formed by SiO_4 tetrahedra, which includes many silica polymorphs (Zhu et al., 2018). Silica exists in many phases based on changes to pH, including crystalline and amorphous phases (Iler, 1979). In crystalline form, silica exists as quartz, which when hydrated forms silicic acid (Bennett, 1991). Silica as the mineral quartz is formed by the deposition of monomeric silica and at high

temperatures, slow rates of precipitation and low levels of supersaturation (White et al., 1956).

Aqueous Chemistry of Silica

In water, silicon binds with four hydroxyl groups forming silicic acid (H_4SiO_4) (Iler, 1979). Alternate names for silicic acid include, orthosilicic acid, monosilicic acid or monomeric silica. It is ubiquitous in natural waters and is a product of mineral weathering (White, 2003). According to Iler (1979), H_4SiO_4 can be found in all-natural aqueous systems. H_4SiO_4 is a weak acid that can be deprotonated twice, making it a diprotic acid (Benjamin, 2002). The dissociation constants for silicic acid are (Milne et al., 2014),

$$(1)\ H_4SiO_4 \rightarrow H_3SiO_4^- + H^+ \quad pK_{a1} = 9.86$$

$$(2)\ H_3SiO_4^- \rightarrow H_2SiO_4^{2-} + H^+ \quad pK_{a2} = 13.14$$

Figure 1 shows the speciation for silicic acid at the pH ranges from 0 to 14. The dominant form of silicic acid that exists in the pH range from 0 to 7 is the protonated, H_4SiO_4 (see Figure 1). Once the pH reaches 9.86, equal amounts of H_4SiO_4 and $H_3SiO_4^-$ exist in solution. As the pH continues to increase, the second pKa is reached at 13.14. Table 1 identifies the silica species in solution calculated using alpha values at pH's 7 -14 shown in Equations 3 to 5:

$$(3)\ \alpha_0 = \frac{[H^+]^2}{[H^+]^2 + [H^+]K_{a1} + K_{a1}K_{a2}}$$

$$(4)\ \alpha_1 = \frac{[H^+]K_{a1}}{[H^+]^2 + [H^+]K_{a1} + K_{a1}K_{a2}}$$

$$(5)\quad \alpha_2 = \frac{K_{a1}K_{a2}}{[H^+]^2+[H^+]K_{a1}+K_{a1}K_{a2}}$$

The equation $\alpha_0 + \alpha_1 + \alpha_2 = 1$ states that the sum of the individual concentration has to equal the total concentration. According to Table 1, at pH 7, the percentage of H_4SiO_4 is nearly 100%. As pH increases less of the H_4SiO_4 species is present. At pH 10, the percentage of H_4SiO_4 and $H_3SiO_4^-$ are about 39% and 61%, respectively. At pH 14, the percentage of $H_3SiO_4^-$ and $H_2SiO_4^{2-}$ are about 13.7% and 87%, respectively.

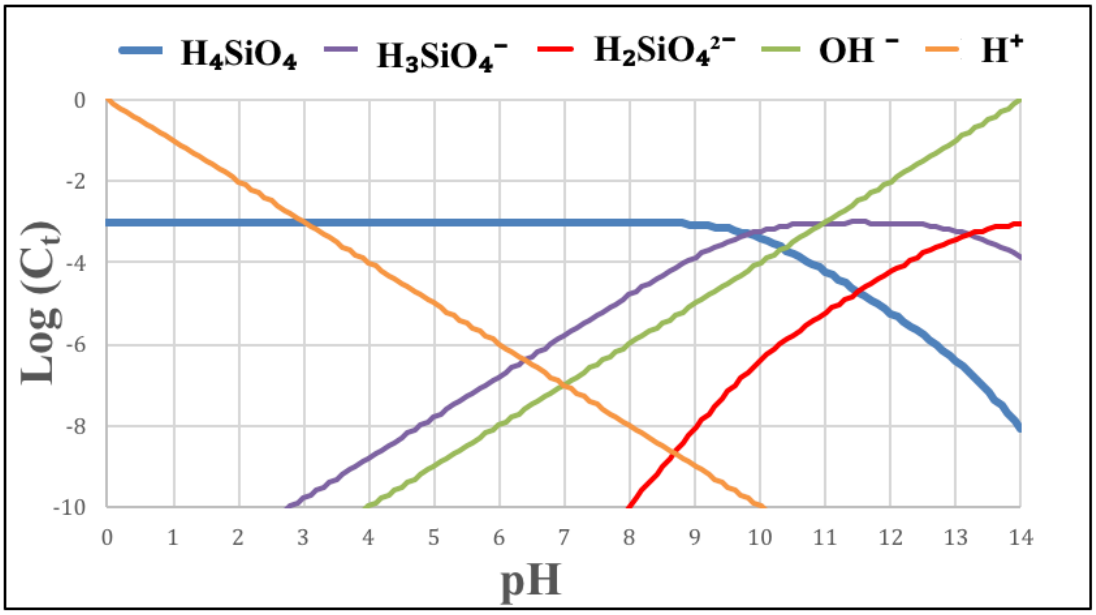

Figure 1: Log C - pH Diagram of Silicic Acid Between pH Values of 0 And 14 for a Total Dissolved Silica Concentration of 10^{-3} M.

pH	H_4SiO_4 (%)	$H_3SiO_4^-$ (%)	$H_2SiO_4^{2-}$ (%)
7	99.8	1.6E-01	9.8E-08
8	98.4	1.6	9.8E-06
9	86.3	13.7	8.6E-04
10	38.7	61.3	3.9E-02
11	5.9	93.5	0.59
12	5.9E-01	93.5	5.9
13	3.9E-02	61.3	38.7
14	8.6E-04	13.7	86.3

Table 1: Silica Speciation From pH 7 to pH 14.

Formation of Silica Scale

Silica scale is described by three physiochemical properties: solubility; pH; and polymerization. The solubility limit of amorphous silica in water at 25 °C is approximately 120 mg/L (Stumm and Morgan, 1996; Sanks, 1978). Silica can precipitate when the reaction quotient (Q = the ratio of the activities of the reaction products by the reactants) is greater than the K_{sp} or when the saturation index ($SI = Log(\frac{Q}{K_{sp}})$) is positive (Benjamin, 2002). When silica concentrations exceed the saturation limit, silica goes through a process called autopolycondensation. Belton et al. (2012) claims that autopolycondensation lowers the concentration of orthosilicic acid, which results in each condensation reaction between two orthosilicic acid molecules generating one water molecule each ($2\,Si(OH)_4 \rightarrow 2\,H_2SiO_3 + 2\,H_2O$).

The formation of amorphous silica deposits occur as the polymerization of silica monomers or silica colloids at high concentrations (Bremere et al., 2000). During the

process of polymerization, silica monomers can form many different silica polymers including dimers, trimers and oligomers. The polymerization reactions differ based on the pH of the water, which dictates what polymers are formed (Baca, 2017). Colloids are particles that stay suspended in solution and therefore they will not settle out (Howe et al., 2012). Additionally, silicate scale is formed when supersaturated meta silicic acid $(H_2SiO_3)_n$ polymerizes to form insoluble colloids or silica gels. (Antony et al., 2011; Gill, 1993). White et al. (1956), found that the rate of polymerization is influenced by parameters such as pH, temperature and the degree of supersaturation.

Silica Scale Formation in Cooling Towers and Thermoelectric Power Plants

The formation of silica scale is a problem for industries that use cooling towers and for closed-loop cooling systems for thermoelectric power plants. For these systems, water is conveyed from a condenser to a cooling tower that is exposed to the atmosphere. The exposure to atmosphere allows the water to cool through evaporation. When the water is recirculated, evaporation causes silica to become concentrated and form a glassy scale on the surface of heat exchangers, furnace tubes, boilers and turbines which may result in a loss of heat transfer efficiency, plugging of small pipes and passages, and the need for cleaning (Batchelor et al., 1991; Dai et al., 2016; Iler, 1974).

Silica Scale Formation in RO Membranes

RO is a membrane treatment process that separates dissolved solutes from water (Howe et al., 2012). In RO, pressurized feed water enters the membrane that is separated by a semipermeable membrane. Water that passes through the membrane is called the permeate stream and is free of solutes. Water retained by the membrane is called the

concentrate stream. As solutes are rejected by the membrane the feed stream becomes more concentrated and the potential for fouling increases (Howe et al., 2012). Silica present in the water will become concentrated in the feed stream. The concentrated silicic acid (H_4SiO_4) may subsequently form scale on the feed side of the membrane. Silica can foul membranes by forming a glassy scale when concentrated by RO causing a need for replacing and an increase in treatment cost (Cob et al., 2014 and Den and Wang, 2008).

Prevention of Scale and Fouling

Many techniques have been examined to prevent the formation of silica scale including adjusting the pH and the addition of scale inhibitors. Filmtec (1995) proposed a 3-step silica mitigation process as follows: (i) maintaining the iron and aluminum concentrations below 0.05 mg/L; (ii) establish a treatment system to remove dissolved and colloidal silica and silicates; and (iii) acidification (pH < 7) of the feed water and frequent acid cleanings.

Removing soluble silica through lime softening, adsorption, co-precipitation, ion-exchange and coagulation/filtration have been used. This research did not consider ion-exchange and coagulation/filtration methods because the focus was to gain a better understanding of and to capitalize on the laboratory techniques used by Sims (2015), Baca (2017) and Sasan et al. (2017).

Scale Inhibitors

Scale inhibitors are one method of preventing silica scale. In industrial equipment, Kemmer and McCallion (1979) suggested maintaining silica concentrations in high pressure boilers below 8 mg/L and 22 μg/L in steam turbines. With such low

silica concentrations, industries needed to find a solution. Scale inhibitors were developed by company's such as King Lee Technologies and NALCO. Scale inhibitors keep silica suspended in solution past the saturation point which prolongs the formation of silica scale. Scale inhibitors can cause either inhibition or dispersion. Inhibition stops the formation of crystals or particles from forming and dispersion keeps scale particles from attaching to a membrane surface, heat exchanger, etc. (Neofotistou and Demadis, 2004).

pH Adjustments

Adjusting the pH is another method that is used to prevent the formation of silica scale. High Efficiency Reverse Osmosis (HERO^{TM}) is a patented process that utilizes the correlation between the pH and the solubility of silica. The HERO^{TM} process begins by passing water through a weak acid cation exchange to remove cations associated with hardness, such as Ca^{2+} and Mg^{2+} (Milne et al., 2014). Then, the pH of the water is raised between 10.3 and 10.5 to increase the solubility of silica before being conveyed through an RO unit (Milne et al., 2014). Overall, the HERO^{TM} process removes divalent cations and increases pH in order to increase RO recoveries and prevent membrane fouling.

Lime Softening

One method used to remove silica from water is hydrated calcium hydroxide or lime. The process is termed lime softening and is normally intended to remove the hardness from water. The presence of divalent cations, such as calcium (Ca^{2+}) and magnesium (Mg^{2+}) found in water, define the term hardness. During lime softening, calcium hydroxide is added to raise the pH and precipitate calcium carbonate ($CaCO_3$) and magnesium hydroxide ($Mg(OH)_2$) (Roalson et al., 2003; Al-Mutaz and Al-Anezi,

2004). The resulting precipitates are then removed by either filtration or sedimentation (Al-Mutaz and Al-Anezi, 2004). According to Roalson et al. (2003), the following equations show the solubility reactions for calcium and magnesium:

$$(6)\ CaCO_3\,(s) = Ca^{2+} + CO_3^{2-}\quad K_{sp,Ca} = 10^{-8.48}$$

$$(7)\ Mg(OH)_2(s) = Mg^{2+} + 2\,OH^-\quad K_{sp,Mg} = 10^{-11.16}$$

Al-Mutaz and Al-Anezi (2004) describes four major objectives of lime softening as: (a) removal of CO_2, (b) removal of carbonate hardness, (c) removal of calcium non-hardness and (d) removal of magnesium non-carbonate hardness. Additionally, according to Al-Mutaz and Al-Anezi (2004), during lime softening the silica concentrations are decreased due to the silica molecules attaching to the surface of the precipitated magnesium ions at high pH values. It was discovered that the removal of silica through lime softening is dependent on the amount of $Mg(OH)_2$ precipitate formed during the process (Montgomery, 1985). Masarwa et al. (1997) showed that in conditions where $Mg(OH)_2$ precipitates are low in the lime softening process the addition of preformed $Mg(OH)_2$ improves silica removal.

Magnesium Hydroxide

Many studies have examined the role of magnesium in silica removal. Some researchers suggest that silica is removed through a co-precipitation process (Cob et al., 2014). The co-precipitation process involves the formation of the amorphous $Mg(OH)_2$ to which silica is adsorbed. Figure 2 shows a Log C - pH diagram for the concentration of Mg^{2+} ion in equilibrium with amorphous $Mg(OH)_2$. The green line shows the

concentration of Mg^{2+} at equilibrium with the solid $Mg(OH)_2$. If the concentration of Mg^{2+} is above the green line, the solution is supersaturated, and precipitation can occur. If the concentration is below the green line, the solution is undersaturated and precipitation will not occur.

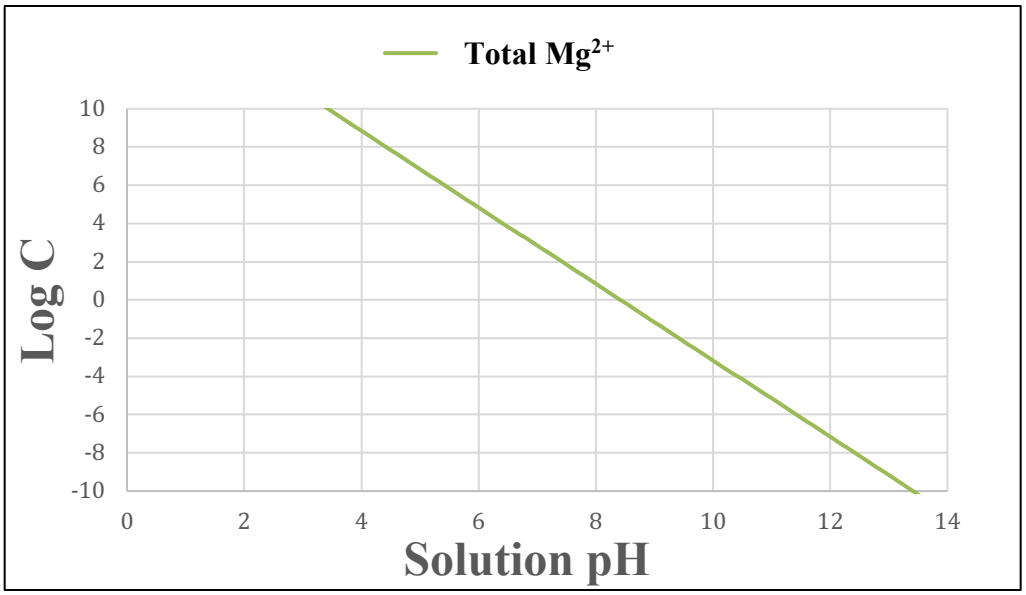

Figure 2: Log C - pH Diagram for Insoluble Magnesium Hydroxide.

Other researchers claim magnesium hydroxide uses an adsorption mechanism to remove the silica from water (Sheikholeslami et al., 2001). The adsorption mechanism involves the preforming of the precipitate and introducing it to silica in the water. In a study completed by Latour et al. (2014), dosing with a magnesium hydroxide concentration of 1500 mg/L and pH 11.5, 86% of the silica was removed. This indicates that in the absence of calcium, preformed magnesium can remove silica by serving as an adsorbent. Sims (2015), completed her thesis on silica's removal mechanism by adding freshly precipitated magnesium hydroxide to a solution containing approximately 65 mg/L of silica. Using this technique, about 90% silica removal was achieved at a dose of 1,000 mg/L as Mg^{2+} and initial pH of 10.51 The co-precipitation mechanism was

dismissed due to limited silica removal (~30%) when compared to freshly precipitated magnesium hydroxide at the same dose and initial pH. This would suggest then that the favored mechanism is adsorption.

As the literature suggests, $Mg(OH)_2$ is a good adsorbent for silica at a pH of 9.5 or greater (Sims, 2015; Sheikholeslami et al., 2001; Cob et al., 2014). Magnesium hydroxide removes silica by forming magnesium silicates. Magnesium silicates are formed because silicic acid begins to deprotonate at pH 9 (see Table 1) and the negative charge on $H_3SiO_4^-$ allows it to bind to the $Mg(OH)_2$. Wang et al. (2010) discovered a magnesium silicate chemical formula of $Mg_3Si_4O_{10}(OH)_2$.

Ferric Hydroxide

Ferric hydroxide was found to remove silica via adsorption (Iler, 1974). According to Yokoyama et al. (1980), the adsorption and surface polymerization of silicic acid onto ferric hydroxide surfaces were at a maximum at pH 9. McKeagure (1962) found that with an initial silica concentration of 56 mg/L and 500 mg dose of ferric hydroxide, 99.8% silica removal was achieved. Baca (2017), set out to remove silica using performed ferric hydroxide. His initial silica concentration was 125 mg/L and the ferric hydroxide had a removal efficiency of 90%. His findings suggested that ferric hydroxides can remove silica at both acidic and basic pH's which could be advantageous for the treatment of waters with high silica concentrations. This differs from the calcium hydroxide and magnesium hydroxide because they precipitate at higher pH's.

Similar to magnesium, Iron(III) has also been shown to remove silica via co-precipitation (Aljohani, 2016). This process involves the formation of amorphous

$Fe(OH)_3$ with subsequent adsorption of silica onto the solid phase. Figure 3 shows a Log C - pH diagram for the concentration of Iron(III) species in equilibrium with amorphous $Fe(OH)_3$. If the concentration of Iron(III) is above the green U shape, the solution is supersaturated, and $Fe(OH)_3$ precipitation can occur. If the concentration is below the green U shape, the solution is undersaturated.

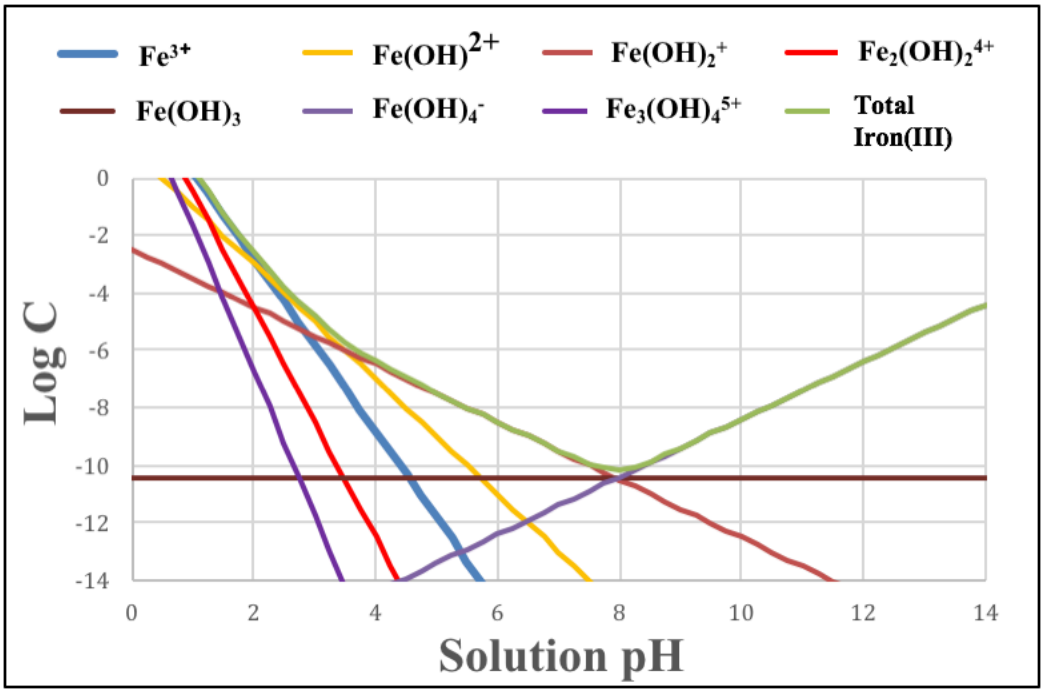

Figure 3: Log C - pH Diagram for Iron(III) Species in Equilibrium with $Fe(OH)_3$.

Aluminum Hydroxide

Figure 4 shows a Log C - pH diagram for the concentration of aluminum species in equilibrium with amorphous $Al(OH)_3$. If the concentration of aluminum is above the green U shape, the solution is supersaturated, and $Al(OH)_3$ precipitation can occur. The following is the chemical equation for the formation of aluminum hydroxide:

$$(8)\ AlCl_3 + 3\,NaOH \leftrightarrow Al(OH)_3(s) + 3\,NaCl$$

Trivalent ions, such as $Al^{3+,}$ have been shown to decrease solubility and increase silica polymerization (Iler, 1974). Additionally, silica has been shown to have an affinity for aluminum (Gabelich et al., 2005). Many different aluminosilicate minerals exist, such as andalusite, zeolite and topaz. Tokoro et al. (2014), compared the co-precipitation and adsorption mechanisms by which aluminum compounds remove silicates. The findings concluded that at pH 9 the co-precipitation mechanism had a higher silica removal efficiency than the adsorption mechanism at silica concentrations of 0.71 mM and 1.78 mM (Tokoro et al., 2014). Furthermore, Cob et al. (2014) found at pH 8.5, 99.9% silica removal was achieved with 400 mg/L Al^{3+} dose.

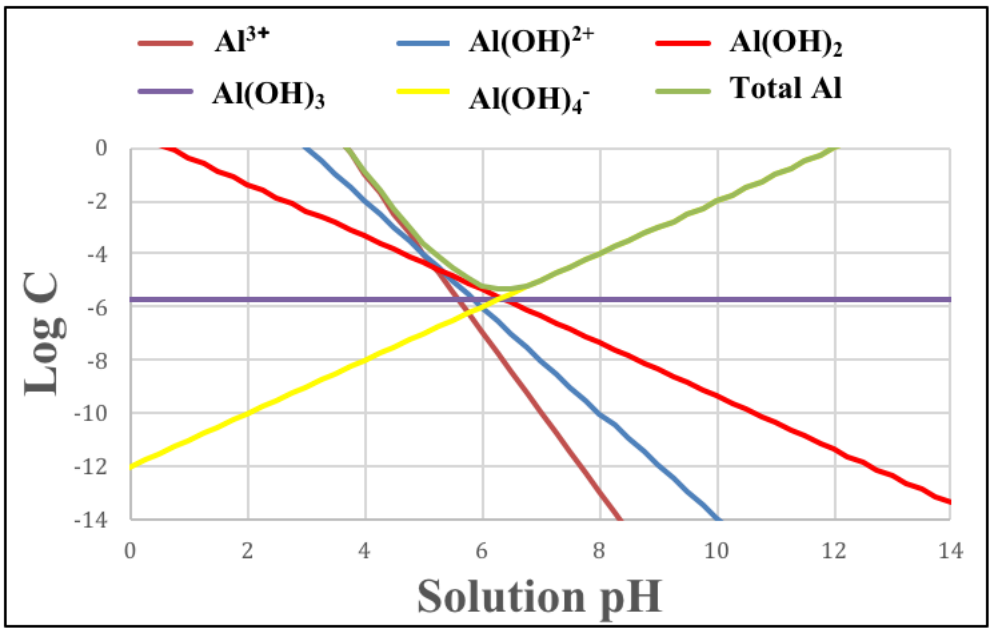

Figure 4: Log C - pH Diagram for Al Species in Equilibrium with $Al(OH)_3$.

Hydrotalcite

A relatively new material used for the removal of silica is hydrotalcite (HTC). The chemical formula of HTC is $Mg_6Al_2(CO_3)(OH)_{16} \bullet 4H_2O$. HTC is a layered network of infinite sheets formed by Mg^{2+} and Al^{3+} ions in an octahedral orientation (Baskaran et al., 2015). The sheets are layered upon each other and contain water and anions such as Cl^-, NO_2^- and CO_3^{2-} in the interspace (Baskaran et al., 2015). One of the earliest studies of silica removal by HTC was Schutz and Biloen (1987). Schutz and Biloen (1987) found that silicic acid polymerized on the HTC structure using a microprobe analysis. They discovered that the Cl^- anion was being replaced by silica, forming a silicate intercalated material (Schutz and Biolen, 1987). Rocha et al. (1999), confirmed this finding using FT-IR spectra. They discovered that the HTC-silicate material showed Si-O-Si peaks occurring at 950-1200 cm^{-1}, meaning silicate units were present on the HTC and at various polymerization states (Rocha et al., 1999). Sasan et al. (2017), compared calcined HTC to uncalcined HTC in the removal of silica from industrial waters. Sasan et al. (2017), discovered that at initial pH 7, 0.82 mM calcined HTC could remove 90% of silica while 0.82 mM uncalcined HTC removed about 10% of silica from the industrial water. It was identified that the surface area of the calcined HTC (~138 m^2/g) was much larger than the uncalcined HTC (~12 m^2/g), resulting in more binding sites for the silica and a higher percent removal (Sasan et al., 2017). Overall, calcined HTC is superior to uncalcined HTC at removing silica in industrial waters.

Discussion on Adsorption vs Surface Precipitation

Adsorption is a type of water treatment that is described as the concentration of dissolved species on the solid surface by chemical reaction or physical attraction to the

surface (Howe et al., 2012). The point of zero charge (PZC) is commonly used when describing adsorption. The PZC is the pH at which the surface of a material is neutral (Benjamin, 2002). When the pH is below the PZC, then the surface is positive. Conversely, if the pH is above the PZC, then the surface is negative.

Surface precipitation, according to Stumm and Morgan (1996), involves ions (which adsorb to the surface of a mineral) precipitating with the constituent ions of the mineral at high surface coverages. In surface precipitation, as the concentration of the sorbate increases, the surface complex concentration and mole fraction of the surface precipitate both increase until the sites on the surface become saturated (Stumm and Morgan, 1996). Typically, surface precipitation is the dominate mechanism at high sorbate/sorbent ratios (Stumm and Morgan, 1996).

CHAPTER 3: MATERIALS AND METHODS

Chapter 3 presents the materials and methods used in this study. This thesis investigated how parameters such as chemical adsorbent, dose and pH affects silica removal from water. This work was comprised of both batch and flow through experiments and used the following adsorbents: freshly precipitated $Mg(OH)_2$, freshly precipitated $Fe(OH)_3$ and calcined HTC. The batch experiments involved equilibrium and kinetic testing of the three adsorbents. With the information obtained in the batch tests, the flow through experiments were used to determine the design parameters including dose and pH for the three materials.

The objectives of this research were as follows:

Objective 1: To investigate and compare the dose of the freshly precipitated $Mg(OH)_2$, freshly precipitated $Fe(OH)_3$ and calcined HTC required to achieve similar removal efficiency for silica.

Objective 2: To investigate and compare the pH of the freshly precipitated $Mg(OH)_2$, freshly precipitated $Fe(OH)_3$ and calcined HTC required to achieve similar removal efficiency for silica.

Objective 3: To investigate and compare the sorption density of silica on freshly precipitated $Mg(OH)_2$, freshly precipitated $Fe(OH)_3$ and calcined HTC at equilibrium to determine the adsorption isotherm and isotherm parameters.

Objective 4: To investigate and compare the kinetics of silica sorption onto freshly precipitated $Mg(OH)_2$, freshly precipitated $Fe(OH)_3$ and calcined HTC.

Objective 5: Propose a mechanism for how HTC removes silica.

Objective 6: Determine design parameters for the flow through experiments such as dosage, pH and hydraulic residence time.

Materials

Preparation of Source Water

RO concentrate water was generated by GE Osmonics RO Unit (RO Unit) (Figure 5) at the University of New Mexico. A hose was used to connect a tap water source to the RO Unit. The tap water entered the RO unit and passed through 3 RO membranes. The concentrate stream had a silica concentration of about 124 mg/L and pH of 8.34. Triplicate samples of the RO concentrate water were tested for cation and anion concentrations using Inductively Coupled Plasma Optical Emission Spectrometry (ICP-OES) and Ion Chromatography (IC). The TDS of the RO concentrate water was 364.60 mg/L. The averaged results can be seen in Table 2.

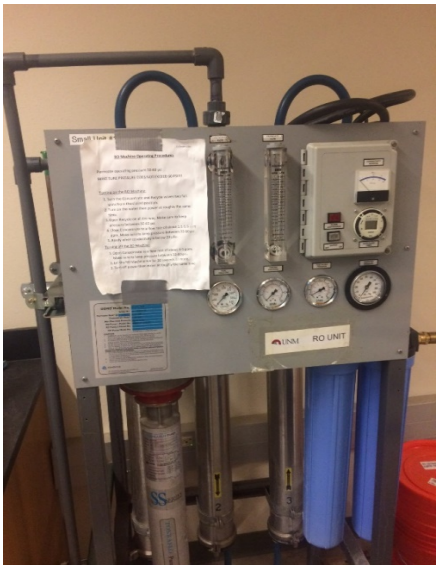

Figure 5: GE Osmonics RO Unit.

ICP-OES			IC		
Cation	**Average Concentration (meq/L)**	**Average Concentration (mg/L)**	**Anion**	**Average Concentration (meq/L)**	**Ave Concentration (mg/L)**
Ba^{2+}	0.00313	0.215	F^-	0.081	1.54
Ca^{2+}	2.66	53.2	Cl^-	1.73	61.26
Cd^{2+}	0.0000587	0.0033	NO_2^-	0.035	1.61
Li^+	0.026	0.183	Br^-	0.00768	0.6141
Mg^{2+}	1.37	16.72	NO_3^-	0.044	2.73
Na^+	3.85	88.56	SO_4^{2-}	2.85	137
Sr^{2+}	0.0219	0.96			
∑ Cations = 7.9 meq/L, 159.8 mg/L			∑ Anions = 4.7 meq/L, 204.75 mg/L		

Table 2: RO Concentrate Water Composition.

Preparation of Stock Solutions

Three stock solutions were prepared for the experiments. Stock solution #1 was a 1 M magnesium chloride ($MgCl_2$) solution. To prepare stock solution #1, 95.211 g of high purity $MgCl_2$ from AMRESCO was weighed on an analytical balance and dissolved into DI water and diluted to 1 L in a volumetric flask. The reaction between the $MgCl_2$ and the DI water was exothermic and therefore the vessel was submerged in a water bath to cool. Stock solution #2 was a 1 M ferric chloride ($FeCl_3$). Stock solution #2 was made using 270 g of $FeCl_3$ from JT Baker which was dissolved into DI water and diluted to 1 L in a volumetric flask. Finally, stock solution #3 was a 1 M sodium hydroxide (NaOH). To generate stock solution #3, 40 g of NaOH from AMRESCO was dissolved into 1 L of

DI water. This reaction was also exothermic as well, so the water bath was used to cool the vessel.

A summary of the compositions of each of the stock solutions can be seen in Table 3:

Stock Solution	Chemical Formula	Molecular Weight (g/mol)	Stock Concentration (M)	How much chemical to add (g/L)
#1	$MgCl_2$	95.211	1	95.211
#2	$FeCl_3$	270	1	270
#3	NaOH	40	1	40

Table 3: Composition of Stock Solutions.

Preparation of Adsorbents

To maintain consistency in the removal mechanism of silica, all adsorbents were formed/measured in the same fashion.

Magnesium Hydroxide

The equation to make magnesium hydroxide ($Mg(OH)_2$ (s)) from $MgCl_2$ and NaOH is shown in Equation 9.

$$(9)\ MgCl_2 + 2\,NaOH \rightarrow Mg(OH)_{2\,(s)} + 2\,NaCl$$

As a result of Equation 9, the molar ratio of $MgCl_2$ to NaOH was 1:2. Using the prepared stock solutions, a ratio of one part of Stock Solution #1 to two parts of Stock Solution #3 was used or in other words the amount of NaOH was twice the amount of $MgCl_2$. The

pH of the precipitation reaction was always 10 or higher and the $Mg(OH)_2$ was used wet for silica removal. In order for the chemicals to fully precipitate, the reaction was completely mixed on a stir plate until a white cloudy precipitate was seen. Table 4 illustrates how the $Mg(OH)_2$ was made.

Equation Used	Variables	Algebra	Results
Concentration = C Volume = V $C_1.V_1 = C_2.V_2$	C_1 = 1 M $MgCl_2$ V_1 = Solve for this C_2 = 0.003 M $MgCl_2$ V_2 = 50 mL	$V_1 = \frac{C_2 V_2}{C_1}$ $V_1 = \frac{0.003\ M\ X\ 50\ mL}{1M}$	V_1 = 0.15 mL $MgCl_2$ Therefore, 0.15 mL X 2 = 0.30 mL NaOH and diluted to 50 mL with DI

Table 4: Equations Used to Prepare $Mg(OH)_2$.

Ferric Hydroxide

The model for making ferric hydroxide ($Fe(OH)_3$ (s)) from $FeCl_3$ and NaOH is shown in Equation 10 as follows:

$$(10)\ FeCl_3 + 3\ NaOH \rightarrow Fe(OH)_{3\ (s)} + 3\ NaCl$$

As shown in Equation 10, the molar ratio of $FeCl_3$ to NaOH was 1:3. Using the prepared stock solutions, a ratio of one part of Stock Solution #2 to three parts of Stock Solution #3 was used. The pH of the precipitation reaction was always 10 or higher and the

$Fe(OH)_3$ was used wet for silica removal. When this ratio is completely mixed, it produces a deep, dark brown precipitate. Table 5 illustrates how the $Fe(OH)_3$ was made.

Equation Used	Variables	Algebra	Results
Concentration = C Volume = V $C_1.V_1 = C_2.V_2$	C_1 = 1 M $FeCl_3$ V_1 = Solve for this C_2 = 0.003 M $FeCl_3$ V_2 = 50 mL	$V_1 = \frac{C_2 V_2}{C_1}$ $V_1 = \frac{0.003\ M\ X\ 50\ mL}{1M}$	V_1 = 0.15 mL $FeCl_3$ Therefore, 0.15 mL X 3 = 0.45 mL NaOH and diluted to 50 mL with DI

Table 5: Equations Used to Prepare $Fe(OH)_3$.

Hydrotalcite

The Hydrotalcite (HTC), which comes in the form of a powder, was purchased by Sandia National Laboratories from Sigma-Aldrich and was activated by calcifying at 500 °C. To convert from mass concentrations to molar concentrations the mass was divided by the molecular weight (603.98 g/mol). According to Sasan et al. (2017), when the HTC is calcified, the surface area increases from around 12 m^2/g to about 138 m^2/g allowing for greater adsorption for silica. The formation of HTC is shown in the Equation 11 as follows.

$$(11)\ Mg_6Al_2(OH)_{16}(CO_3).4H_2O \rightarrow 5MgO.MgAl_2O_4 + CO_2 + H_2O$$

Analytical Methods

Silica Concentration

The silica concentration was tested by the Silicomolybdate Method. To complete this method, a High Range 10 mL SiO_2 Reagent Hach test was used. The DR/890 Colorimeter (Figure 6) measured silica concentrations ranging from 1 mg/L – 100 mg/L.

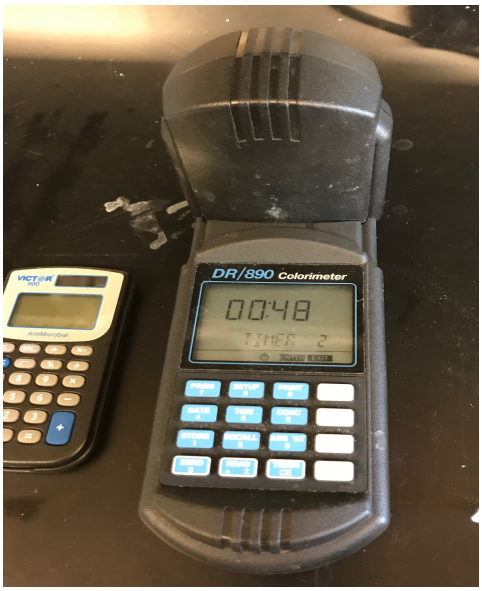

Figure 6: DR/890 Colorimeter Reader.

Due to the high silica concentrations (approximately 124 mg/L) found in the RO concentrate water, the final 10 mL sample was diluted 1:1 with 5 mL of DI water in addition to 5 mL of the filtered RO concentrate water. Pall Corporation Mixed Cellulose Esters Membrane 0.22 µm was used to filter the RO water (Figure 7).

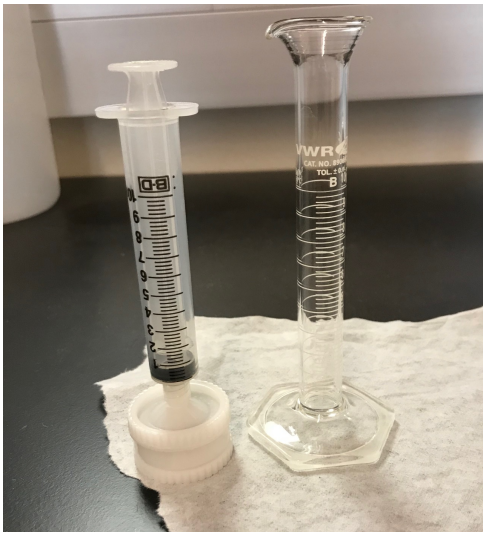

Figure 7: Sample Filtration Setup.

Figure 8 shows the inside of the filter with the adsorbents filtered. The Hach tests were performed by adding Molybdate and the Acid Reagent to the 10 mL vial. The chemicals mix together for 10 minutes so they can completely dissolve. While dissolving, the 10 mL solution will turn yellow due to the bonding of Molybdosilicate and Phosophomolybdic acid.

Figure 8: $Fe(OH)_3$ Filtered by the Pall Corporation Membrane.

The yellow color corresponds to the amount of silica in the solution; therefore, brighter and stronger colors of yellow will have more silica present. Figure 9 shows a progression of yellow colors starting with the strongest on the left and lighter colors moving to the right. This means the highest silica concentrations were found in the 10 mL sample found on the left. When the 10-minute period was over, and the chemicals were dissolved, the citric acid reagent was added to the vial to break the bonds of the Phosophomolybdic and then was dissolved for two minutes. The DR/890 Colorimeter reader was set to read SiO_2 (Program 89). The Hach Test is a colorimetric test; therefore, a clear 10 mL DI water sample must be run to zero the test out. After the reader was zeroed, each of the tests were run and the results recorded.

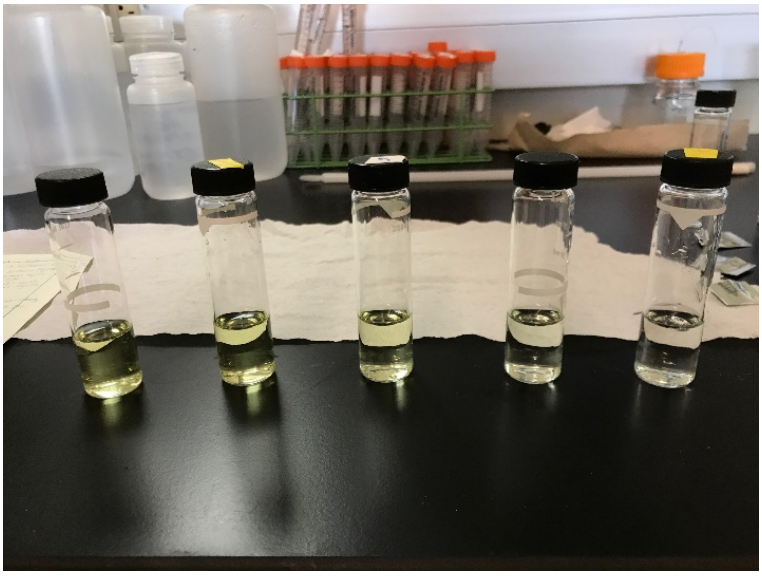

Figure 9: Results of Hach Test.

pH

The instrument used for measuring pH was Fisher Scientific accumet® pH Reader. Calibration was completed by removing the glass Electrode from the vial of 3.5 M KCl located on the tip of the probe. The pH probe was calibrated using standard

buffers of pH's of 4.01, 7.0 and 10.01, respectively and once the pH reader reads "ready", the pH of the solution was measured.

Batch Test

Initial silica concentration and final pH were two important variables that were considered when using the RO concentrate. Due to the presence of Ca^{2+} and Mg^{2+} ions in the RO concentrate (Table 2), blank samples were run to determine if the removal of silica might have occurred by the precipitation of the Ca^{2+} and Mg^{2+} ions when the pH was raised. To complete the batch tests, the pH of the RO concentrate was raised using 1 M NaOH to the desired pH value and the initial silica concentration was measured. Then in the next step, the pH of the RO concentrate was lowered using 1 M HCl and the chemical doses were added.

The RO concentrate had an initial silica concentration of 124 mg/L. The results of the blank samples showed that at pH 9, the final silica concentration was 124 mg/L; at pH 10 it was 112 mg/L; at pH 11 it was 105 mg/L; and pH 12 it was 95 mg/L. The values measured were used for the initial silica concentrations in order to neglect the effect of the co-precipitating ions.

Additionally, to achieve the desired final pH value, preliminary experiments were completed that compared the results of the initial pH versus the final pH of the RO concentrate water with the addition of the adsorbent doses for 24 hours. Using these results, the pH was adjusted using 1 M HCl to achieve the final pH.

Objective 1: The Effect of Dose on Silica Removal

Experiments 1 through 3 compared the silica removal of freshly precipitated $Mg(OH)_2$, freshly precipitated $Fe(OH)_3$ and calcined HTC on a molar basis. Three

experiments were completed, each used one material, a single final pH value of 10 and 4 doses, for a total of 4 tubes (3 mM dose used 1 tube, 10 mM dose used 1 tube, 30 mM dose used 1 tube and 100 mM dose used 1 tube). Table 6 displays the parameters used for each of the experiments.

The Effect of Dose on Silica Removal						
Exp. No.	**Material**	**pH**	**Doses**			
1.	$Mg(OH)_2$	10	Tube 1 3 mM	Tube 2 10 mM	Tube 3 30 mM	Tube 4 100 mM
2.	$Fe(OH)_3$	10	Tube 1 3 mM	Tube 2 10 mM	Tube 3 30 mM	Tube 4 100 mM
3.	HTC	10	Tube 1 3 mM	Tube 2 10 mM	Tube 3 30 mM	Tube 4 100 mM

Table 6: Summary of Parameters Used in Experiments 1 Through 3.

To complete these experiments, adsorbent doses were added to 12 centrifuge tubes. Of the 12 centrifuge tubes, 4 were dosed with the $Mg(OH)_2$ (Experiment 1.), 4 were dosed with $Fe(OH)_3$ (Experiment 2.) and 4 were dosed with calcined HTC (Experiment 3.). The $Mg(OH)_2$ and $Fe(OH)_3$ were preformed and then centrifuged (see Figure 10) for 30 minutes and the supernatant was decanted. The HTC was weighed on an analytical scale. Then 12 separate 50 mL tubes containing RO concentrate water (the pH was raised to 10 using 1 M NaOH, initial silica concentrations were measured and then in the next step the pH was lowered using 1 M HCl, so the desired final pH could be

achieved) were poured into the initial 12 centrifuge tubes which contained the preformed, decanted doses. The tubes were then put on a VWR (DS2-500-1) Orbital Shaker table at 190 rpm for 24 hours. After 24 hours, pH was measured and each of the samples were filtered with Pall Corporation 0.22 µm filters and tested for final silica concentration.

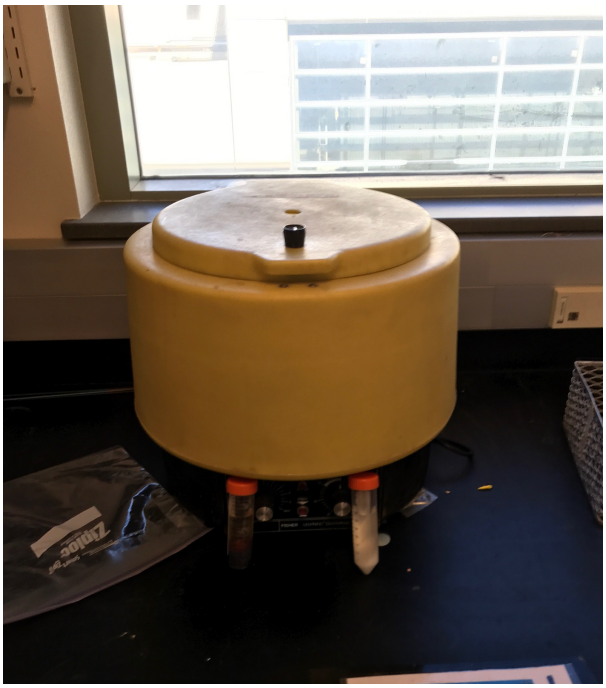

Figure 10: Centrifuge Used for Experiments.

Objective 2: The Effect of pH on Silica Removal

Experiments 4 through 6 examined the silica removal abilities of freshly precipitated $Mg(OH)_2$, freshly precipitated $Fe(OH)_3$ and calcined HTC across various pH values. Three experiments were completed, each using one material, a sorbent dose of 3 mM and 3 pH values, for a total of 3 tubes (pH 9 used 1 tube, pH 10 used 1 tube, pH 11 used 1 tube). Table 7 shows the desired parameters used for each experiment.

The Effect of pH on Silica Removal			
Experiment No.	**Material**	**Dose**	**Final pH**
4.	$Mg(OH)_2$	3 mM	Tube 1 pH 9
			Tube 2 pH 10
			Tube 3 pH 11
5.	$Fe(OH)_3$	3 mM	Tube 1 pH 9
			Tube 2 pH 10
			Tube 3 pH 11
6.	HTC	3 mM	Tube 1 pH 9
			Tube 2 pH 10
			Tube 3 pH 11

Table 7: Summary of Parameters Used in Experiments 4 Through 6.

To complete these experiments, adsorbent doses were added to 9 centrifuge tubes. Of the 9 centrifuge tubes, 3 were dosed with $Mg(OH)_2$ (Experiment 4.), 3 were dosed with $Fe(OH)_3$ (Experiment 5.) and 3 were dosed with HTC (Experiment 6.). The $Mg(OH)_2$ and $Fe(OH)_3$ doses were preformed in separate centrifuge tubes. The preformed doses were centrifuged for 30 minutes and decanted. The HTC was weighed on an analytical scale. Next, in separate tubes containing 50 mL of RO concentrate water the pH was raised using 1 M NaOH to the desired pH values (pH 9, 10 and 11 for each material) and the initial silica concentration was measured. Then, the pH was lowered using 1 M HCl, so the desired final pH could be achieved. Finally, the 50 mL tubes that contained the RO concentrate water were poured into the centrifuge tubes which contained the adsorbent doses. The tubes were then put on a VWR (DS2-500-1) Orbital Shaker table at 190 rpm for 24 hours. After 24 hours, the final pH and silica

concentration was measured using the DR/890 Colorimeter and High Range Silica 10 mL Hach test kits.

Objective 3: Isotherm Testing

Experiments 7 through 9 examined the sorption density of silica on freshly precipitated $Mg(OH)_2$, freshly precipitated $Fe(OH)_3$ and calcined HTC at equilibrium to determine the most applicable isotherm models (Langmuir or Freundlich) and identify isotherm parameters. Three experiments were completed, each using one material, 3 final pH values and 5 doses, for a total of 15 tubes (pH 9 used 5 tubes, pH 10 used 5 tubes, pH 11 used 5 tubes). This was completed three times with each material. Table 8 displays the desired parameters.

Isotherm Testing							
Exp. No.	**Final pH**	**Material**	**Dose**				
7.		$Mg(OH)_2$ (mM)					
	10		Tube 1 3 mM	Tube 2 15 mM	Tube 3 30 mM	Tube 4 45 mM	Tube 5 80 mM
	11		Tube 6 3 mM	Tube 7 15 mM	Tube 8 30 mM	Tube 9 45 mM	Tube 10 80 mM
8.	9	$Fe(OH)_3$ (mM)	Tube 1 3 mM	Tube 2 5 mM	Tube 3 10 mM	Tube 4 15 mM	Tube 5 20 mM
	10		Tube 6 3 mM	Tube 7 5 mM	Tube 8 10 mM	Tube 9 15 mM	Tube 10 20 mM
	11		Tube 11 3 mM	Tube 12 5 mM	Tube 13 10 mM	Tube 14 15 mM	Tube 15 20 mM
9.	9	HTC (mM)	Tube 1 0.5 mM	Tube 2 1.5 mM	Tube 3 2 mM	Tube 4 2.5 mM	Tube 5 3 mM
	10		Tube 6 0.5 mM	Tube 7 1.5 mM	Tube 8 2 mM	Tube 9 2.5 mM	Tube 10 3 mM
	11		Tube 11 0.5 mM	Tube 12 1.5 mM	Tube 13 2 mM	Tube 14 2.5 mM	Tube 15 3 mM

Table 8: Summary of Parameters Used in Experiments 7 Through 9.

To complete these experiments, 15 adsorbent doses were added to 50 mL centrifuge tubes. Again, the $Mg(OH)_2$ and $Fe(OH)_3$ doses were preformed in separate centrifuge tubes, centrifuged and the supernatant was decanted. The HTC was measured using an analytical scale. In separate tubes containing RO concentrate water, the pH was raised using 1 M NaOH to pH 9 for 5 tubes, pH 10 for 5 tubes and pH 11 for 5 tubes, totaling 15 tubes. The silica concentration was measured, and the pH was lowered using 1 M HCl to achieve the desired final pH. The preformed doses of $Mg(OH)_2$, $Fe(OH)_3$ and

HTC were added to each of the respective tubes and placed on a VWR (DS2-500-1) Orbital Shaker table which was set at 190 rpm for 24 hours. After 24 hours, pH was tested and each of the samples were filtered with Pall Corporation 0.22 µm filters and the final silica concentration was measured.

Objective 4: Kinetic Testing

Experiments 10 through 12 investigated the rate of silica sorption onto the freshly precipitated $Mg(OH)_2$, freshly precipitated $Fe(OH)_3$ and calcined HTC. Each experiment used one material and 5 different doses, for a total of 5 tubes. Table 9 shows the parameters used in the three experiments.

Kinetic Testing						
Experiment	**Material**	**Doses**				
10.	$Mg(OH)_2$	Tube 1 30 mM	Tube 2 30 mM	Tube 3 30 mM	Tube 4 30 mM	Tube 5 30 mM
11.	$Fe(OH)_3$	Tube 1 15 mM	Tube 2 15 mM	Tube 3 15 mM	Tube 4 15 mM	Tube 5 15 mM
12.	HTC	Tube 1 1.5 mM	Tube 2 1.5 mM	Tube 3 1.5 mM	Tube 4 1.5 mM	Tube 5 1.5 mM

Table 9: Summary of Parameters Used in Experiments 10 Through 12.

To complete these experiments, 5 centrifuge tubes were filled with 50 mL of RO concentrate water. The initial pH and silica concentration was measured in the RO concentrate. In separate centrifuge tubes, adsorbent doses were added, centrifuged and decanted. The tubes containing the RO concentrate water were introduced to the tubes

that contained the adsorbent doses. The tubes were then placed on a VWR (DS2-500-1) Orbital Shaker table at 190 rpm. At 10-minute intervals the tubes were pulled off the shaker table and filtered using Pall Corporation 0.22 μm filters. Hence, samples were taken at after 10, 20, 30, 40, and 50 minutes. The filtered samples were analyzed for final silica concentration.

Objective 5: Silica Removal Mechanism by HTC

Two batch tests were conducted: (1.) Hach Silica Standard and DI water and (2.) RO concentrate water. To complete the batch test, 500 mL of DI water containing 132 mg/L silica was added to a 500 mL beaker. A magnetic stir bar was used to keep the solution mixed. HTC was added to the water and 5 mL aliquots were extracted from the solution and filtered with Pall Corporation 0.22 μm filters at 5, 15, 30 and 60 minutes. The aliquots were added to 10 mL Hach Tests vials which contained 5 mL of DI water. The final SiO_2 concentration was determined. The test was conducted in an analogous fashion with the RO concentrate water.

Flow Through Test

With the results of the parameters tested above, a custom-made flow through adsorption system was designed that allowed for the testing of design parameters such as hydraulic residence time and membrane fouling.

The overall goals of the flow through system were:

- To test the adsorbent capacities on a larger scale system
- To determine whether any of the adsorbents caused membrane fouling

  To determine long term silica removal performance

Design of Flow Through System

The pilot treatment system consisted of a membrane filter with recirculation provided by a 3E-12N Little Giant In-Line Pump. Figure 11 shows a simple schematic of the flow through system.

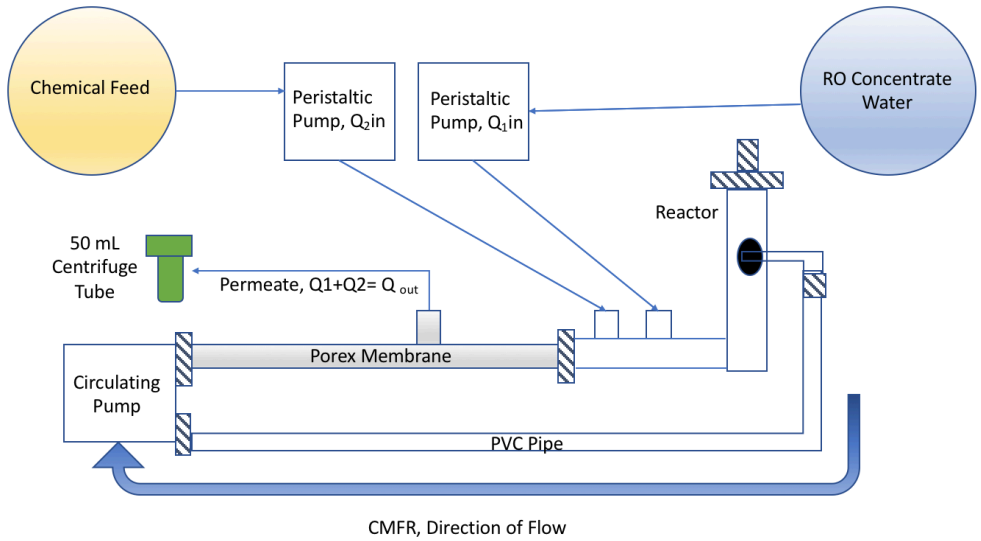

Figure 11: Schematic of the Flow Through System.

The Little Giant Pump recirculated the RO concentrate water and the adsorbents at a rate of approximately 4 gpm (Figure 12). The system also featured a 6-foot, inside-out, 0.1 µm POREX® microfiltration membrane filter (Figure 13). The singular tubular membrane was housed in CPVC with a total active surface area of 0.069 m^2. After each test was completed, the membrane was stored in tap water.

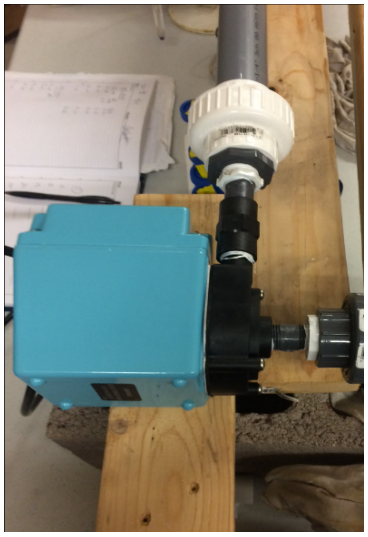

Figure 12: Little Giant Pump.

Figure 13: POREX® membrane.

To startup, the system was first drained to remove the tap water during storage and then refilled with RO concentrate (Table 2) water with a silica concentration of about 124 mg/L. The system, shown in Figure 14, holds a total volume of 2.7 L and acts as a

completely mixed flow reactor (CMFR). The hydraulic residence time (HRT) is the average time the water is in the system (Howe et al., 2012). The HRT involves the flow rate and volume. Equation 12 shows the computation for HRT. The flow rate into the system used was 110 mL/min the system holds a total volume of 2.7 L. Using Equation 12 the HRT resulted in 24.5 minutes.

$$(12)\ HRT = \frac{Volume}{Flow\ Rate}$$

A peristaltic pump was used to fill the system and was connected to the RO concentrate water source. The system was operated for 30-45 minutes to flush out any remaining tap water. When the pH of the permeate was the same as the pH of the RO concentrate water, all of the tap water had been removed. Permeate flow rate was measured with a graduated cylinder and stopwatch. The clear water flux (based on flow in) was approximately 90 $L/m^2 \bullet hr$. Changes in permeate flow and pressure are indicative of membrane fouling.

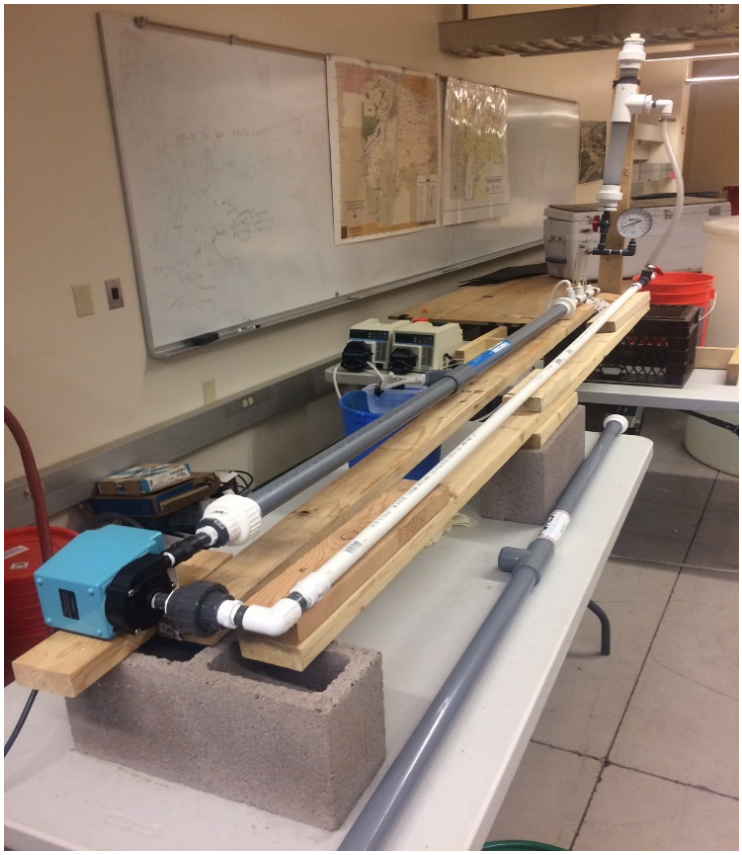

Figure 14: Custom Made Flow Through System.

Objective 6: Continuous Dosing Flow Through Experiments

Experiments 13 through 15 used the data acquired from the batch tests to determine the optimal pH and adsorbent dose. Similar to the batch studies, the $Mg(OH)_2$ and $Fe(OH)_3$ doses were preformed, centrifuged and decanted and the HTC was weighed on an analytical balance. Table 10 shows the parameters used in each experiment.

Continuous Dosing Flow Through Experiments			
Experiment	**Material**	**Dose**	**HRT (min)**
13	$Mg(OH)_2$	19 mM	24.5
14	$Fe(OH)_3$	7 mM	24.5
15	HTC	1.4 mM	24.5

Table 10: Summary of Desired Parameters Used in Experiments 13 Through 15.

In this experiment, fresh adsorbent was introduced to the system every 30 minutes for 5 hours (Table 10). The goal was to maintain a certain percent silica removal for the duration of the experiment. Permeate samples were collected at different time intervals and tested for final silica concentration and final pH.

CHAPTER 4: RESULTS AND DISCUSSION

The purpose of this research was to directly compare three silica removal strategies $Mg(OH)_2$, $Fe(OH)_3$ and HTC and to evaluate the effect of changing design parameters. There were a total of 15 experiments (12 batch and 3 flow through) performed to accomplish the objectives of this research. Objectives 1 and 2 examined the effect of changing the design parameters of dose and pH. Objective 3 investigated and compared the sorption density of silica on freshly precipitated $Mg(OH)_2$, freshly precipitated $Fe(OH)_3$ and calcined HTC at equilibrium to determine the most applicable isotherm. Objective 4 examined the kinetics of silica sorption onto freshly precipitated $Mg(OH)_2$, freshly precipitated $Fe(OH)_3$ and calcined HTC. A proposed mechanism for how HTC removes silica is discussed in Objective 5. Finally, Objective 6 used in the results from the batch experiments to examine design parameters (dose and pH) using the flow-through system.

The Effect of Dose on Silica Removal

Experiments 1 through 3 compared the silica removal capabilities of $Mg(OH)_2$, $Fe(OH)_3$ and HTC for a range of molar doses. Table 11 presents the initial and final pH values for Experiments 1 through 3 (see Chapter 3 regarding pH adjustments). The final pH of 10 was achieved for the preformed doses of $Mg(OH)_2$ and $Fe(OH)_3$. However, for the HTC doses the final pH was always above the desired pH of 10 and were usually above pH 12. As shown in the table, the initial pH value for the 100 mM dose of HTC was lowered to pH 3 and after 24 hours the pH had increased to 12.18. The increase in pH occurs due to the release of OH^- groups from the HTC.

Material	Dose	Initial pH	Final pH
$Mg(OH)_2$	3 mM	8.6	9.74
	10 mM	8.5	10.05
	30 mM	8.34	9.96
	100 mM	8.15	10.25
$Fe(OH)_3$	3 mM	9.98	10.07
	10 mM	9.56	9.78
	30 mM	9.35	9.92
	100 mM	9.2	10.48
HTC	3 mM	3.9	10.9
	10 mM	3.81	11.84
	30 mM	3.13	12.05
	100 mM	3	12.18

Table 11: Summary of pH Results for Experiments 1 Through 3.

Figure 15 summarizes the results showing the percent removal of silica at each of the adsorbent doses at the desired final pH of 10 (see discussion above regarding the final pH of HTC). Figure 15 shows that as the dose is increased for all three materials the percent silica removal is increased. Sims (2015) and Sasan et al. (2017) research also found that increasing the dose of $Mg(OH)_2$, $Fe(OH)_3$ and HTC resulted in increased silica removal. At the 3 mM dose, $Fe(OH)_3$ had approximately 20% higher silica removal than $Mg(OH)_2$ and HTC had 50% higher silica removal than $Fe(OH)_3$. A similar pattern exists for the 10 mM dose. The greatest percent silica removal was achieved with HTC for the 3 mM dose and 10 mM dose. However, the final pH was approximately 12, and the high pH might have contributed to some silica removal through the precipitation of the Mg^{2+} and Ca^{2+} ions. Therefore, it is uncertain whether all the silica removed was due to the HTC. At the 30 mM dose, $Fe(OH)_3$ and HTC had almost 100% removal while the $Mg(OH)_2$

removed around 80%. At the 100 mM dose, nearly 100% silica removal was reached in all three materials.

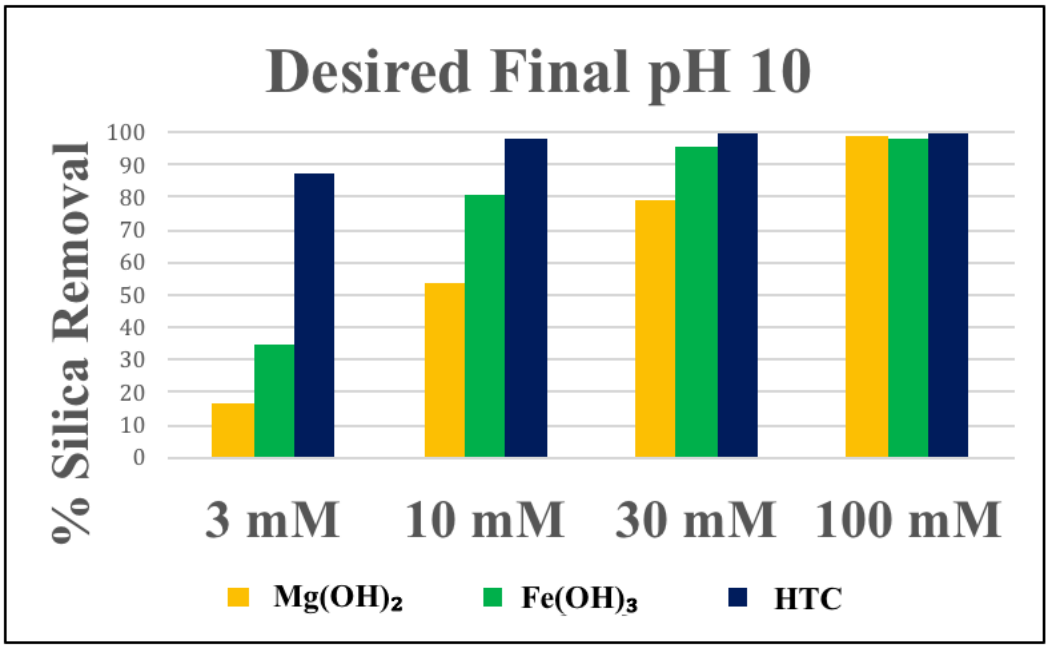

Figure 15: Percent Silica Removal versus Dose at Desired pH 10.

Figure 16 shows the final loading (Q_e) of silica on the solid $Mg(OH)_2$, $Fe(OH)_3$ and HTC. The final loadings are presented in mass of silica per mass of solids to compare the solids on a mass basis. As Figure 16 illustrates, as the dose of the materials is increased, the mass loading is decreased. The largest loading of silica occurred with a 3 mM dose of $Fe(OH)_3$ which was 146 mg/g. At a dose of 10 mM, the $Mg(OH)_2$ and $Fe(OH)_3$ loadings were both approximately 100 mg/g. Comparing Figure 15 to Figure 16, the HTC had the largest percent silica removal but the lowest final loading on a mass basis. In addition, Figure 16 also shows that $Mg(OH)_2$ and $Fe(OH)_3$ had low final loadings and high percent silica removal at the highest dose of 100 mM.

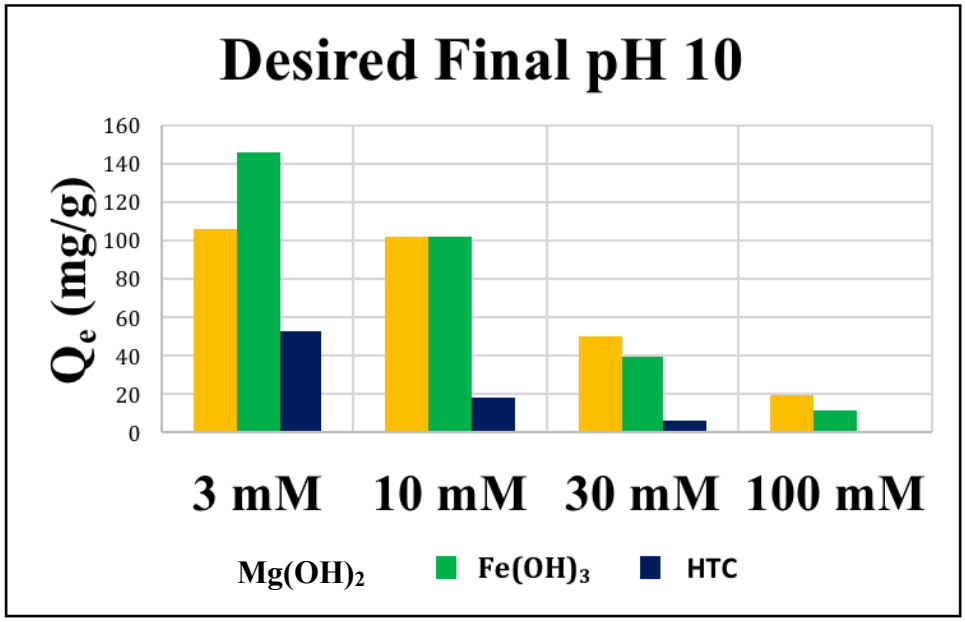

Figure 16: Mass Loading (mg/g) on the $Mg(OH)_2$, $Fe(OH)_3$ and HTC at pH 10.

Figure 17 was constructed to compare the loadings of the solids on a molar basis. This comparison was developed to examine the molar loading because of the large difference in molecular weight across the three adsorbents. The mass concentrations were converted to molar concentrations by multiplying the Mass Loading (Q_e) by the molecular weight of the solid. For example, the Mass loading of $Fe(OH)_3$ was 146 mg/g (at a dose of 3 mM) was multiplied by 106.87 g/mol for a final Molar loading of 15600 mg/mol. The overall trends in the data demonstrate that increasing the dose of the materials leads to decreased molar loadings. At a dose of 3 mM the Molar loading on the HTC was the largest with 32400 mg/mol when compared to the Molar loadings on $Mg(OH)_2$ and $Fe(OH)_3$. At the doses of 30 mM to 100 mM, the Molar loadings (Q_e mg/mol) on each of the solids were similar when compared on a molar basis.

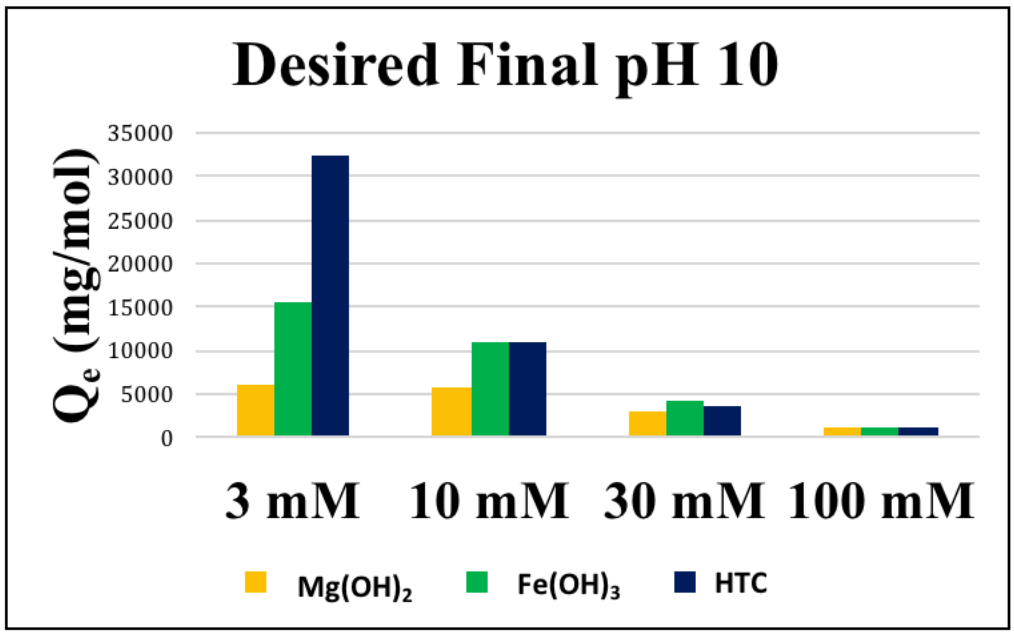

Figure 17: Molar Loading (mg/mol) on the $Mg(OH)_2$, $Fe(OH)_3$ and HTC at pH 10.

The Effect of pH on Silica Removal

Experiments 4 through 6 examined the effect of pH on silica removal. Figure 18 shows the percent removal at a dose of 3 mM for pH 9, 10, and 11 for the $Mg(OH)_2$. The graph illustrates a general trend of increasing pH to an increase of silica removal. The $Mg(OH)_2$ adsorbed the largest amount of silica at pH 11 (18%) and the smallest at pH 9 (11%). However, the percent removal for $Mg(OH)_2$ at a dose of 3 mM were small ranging from around 12% at pH 9 to 18% at pH 11. In other words, $Mg(OH)_2$ is not very effective at removing silica at a dose of 3mM within a pH range of 9 to 11.

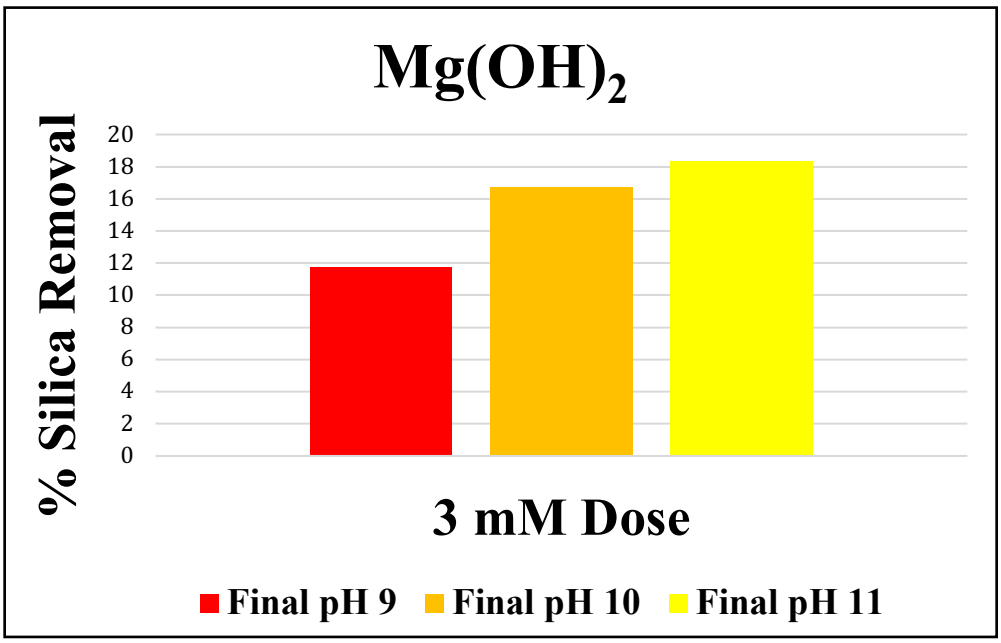

Figure 18: The Percent Silica Removal vs. pH at a 3 mM Dose of $Mg(OH)_2$.

Figure 19 shows the percent removal at a dose of 3 mM for the three pH 9, 10 and 11 for $Fe(OH)_3$. This is a very interesting graph because there is less removal as pH increases from 9 to 11. This is completely opposite of trend shown for $Mg(OH)_2$ in Figure 18. The largest silica removal occurred at pH 9 with 40% removal while at pH 11 the silica removal was 21%.

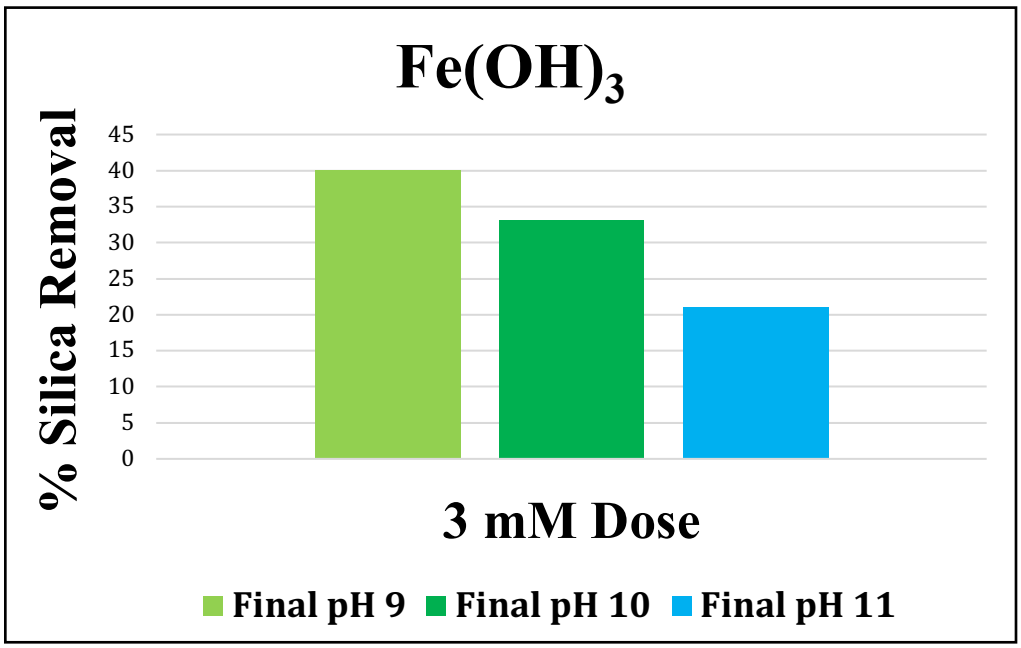

Figure 19: The Percent Silica Removal vs. pH at a 3 mM Dose of $Fe(OH)_3$.

Additionally, when comparing the $Mg(OH)_2$ to $Fe(OH)_3$, the ΔpH from the initial to final pH for the $Mg(OH)_2$ was significantly larger than that of the $Fe(OH)_3$. According to Table 12, at a desired final pH of 9, the initial pH in 3 mM $Mg(OH)_2$ was lowered to 7.54 using 1 M HCl to achieve a final pH of 9.25 while the initial pH was lowered to 9.01 in the $Fe(OH)_3$ to achieve a final pH of 8.82. These experiments reflect that at a dose of 3 mM, the pH for $Fe(OH)_3$ does not change much from initial to final but the pH for $Mg(OH)_2$ must be lowered to achieve the final pH. This was attributed to the dissolution of the $Mg(OH)_2$.

Material	Dose	Initial pH	Final pH
$Mg(OH)_2$	3 mM	7.54	9.25
	3 mM	8.6	9.73
	3 mM	10	10.56
$Fe(OH)_3$	3 mM	9.01	8.82
	3 mM	10.02	10.07
	3 mM	11	10.9
HTC	3 mM	3	12.2
	3 mM	5.06	12.8
	3 mM	8.34	12.3

Table 12: Summary of pH Results for Experiments 4 Through 6.

Theoretical calculations were completed to determine how much Mg^{2+} would dissolve with the addition of the performed $Mg(OH)_2$ doses at the various pH values. Equation 13 identifies how the Mg^{2+} concentrations were calculated at various pH values. The K_{sp} value used was $10^{-11.16}$.

$$(13) \quad K_{sp} = [Mg^{2+}][OH^-]^2$$

The results of the calculations are summarized in Table 13. The concentration of magnesium (mol/L) at pH values 9, 10 and 11 were $10^{-1.16}$, $10^{-3.16}$ and $10^{-5.16}$, respectively.

pH	$[OH^-]^2$	$[Mg^{2+}]$
9	10^{-10}	$10^{-1.16}$
10	10^{-8}	$10^{-3.16}$
11	10^{-6}	$10^{-5.16}$

Table 13: The magnesium concentrations calculated at pH values 9, 10 and 11.

The initial Mg^{2+} concentration ($10^{-3.16}$ M, Table 2) in the RO concentrate water was taken into consideration. To complete the dissolution calculation, the initial magnesium concentration was subtracted from the final magnesium concentrations at pH 9, 10 and 11. The results show that at pH 9, 10^{-2} M would dissolve, at pH 10, 0 M would dissolve and at pH 11, is supersaturated. The dissolution calculations were compared to the doses of preformed $Mg(OH)_2$ to see how much of the $Mg(OH)_2$ would dissolve in the RO concentrate water. Table 14 shows how much of the performed $Mg(OH)_2$ doses would dissolve at the various pH values.

Preformed $Mg(OH)_2$ Dose (mM)	pH 9: (10^{-2} M)	pH 10: (0 M)	pH 11: (Supersaturated)
3 or $10^{-2.5}$	100% Dissolved	0% Dissolved	Supersaturated
10 or 10^{-2}	100% Dissolved	0% Dissolved	Supersaturated
30 or $10^{-1.5}$	33.3% Dissolved	0% Dissolved	Supersaturated
100 or 10^{-1}	10% Dissolved	0% Dissolved	Supersaturated

Table 14: The dissolution of the preformed $Mg(OH)_2$ doses in the RO concentrate water.

According to the calculations regarding dissolution of $Mg(OH)_2$ in the RO concentrate water (see Table 14), at pH 9 the 3 mM and 10 mM dose would completely dissolve in solution resulting in zero silica removal which contradicts the results shown in Figure 18 where about 12% and approximately 18% silica removals were measured after 24 hours. According to Benjamin (2002), when the solution is considered to be undersaturated with respect to the solid and a solid is present, it will dissolve as the system equilibrates. Because $Mg(OH)_2$ is considered to be slightly soluble and 24 hours may not be an adequate amount of time for the dissolution may explain why silica was removed by 3 mM and 10 mM doses at pH 9.

When the doses of $Mg(OH)_2$ at pH 10 were added to the RO concentrate water, the amount of Mg^{2+} in the water was equal to final Mg^{2+} concentration. Hence, the dissolution calculation (see Table 14) resulted in no Mg^{2+} dissolution and the preformed $Mg(OH)_2$ would stay as the precipitate (Figure 15 and Figure 18). For doses tested at pH 11, the calculation showed that the Mg^{2+} concentrations resulted in a supersaturated

solution (Figure 18). Therefore, the preformed $Mg(OH)_2$ will stay in solution as the precipitate.

A similar calculation was performed for the solubility of Fe^{3+} to confirm that no Fe^{3+} will dissolve from the addition of preformed $Fe(OH)_3$. The $Fe(OH)_3$ precipitate was desired for the removal of silica (Figures 15 and Figure 19). Equation 14 displays how the Fe^{3+} concentrations were calculated.

$$(14)\ K_{sp} = [Fe^{3+}][OH^{-}]^3$$

The K_{sp} value used for the calculation was 6.0×10^{-38}. The results of the calculations are summarized in Table 15. The concentration of iron(III) (mol/L) at pH values 9, 10 and 11 were $10^{-22.22}$, $10^{-25.22}$ and $10^{-28.22}$, respectively.

pH	$[OH^-]^3$	$[Fe^{3+}]$
9	10^{-15}	$10^{-22.22}$
10	10^{-12}	$10^{-25.22}$
11	10^{-9}	$10^{-28.22}$

Table 15: The iron(III) concentrations determined at pH values 9, 10 and 11.

According to Table 2 in Chapter 3, no Fe^{3+} was present in the RO concentrate water. Based on the results of the calculation, the addition of $Fe(OH)_3$ at the pH and doses tested would remain in the RO concentrate water as a precipitate.

Figure 20 displays the percent removal at a dose of 3 mM HTC at an initial pH 3, 5 and 8.34. As the initial pH value was increased for the HTC, the silica removal was approximately 90% for all pH values. Therefore, no trends in silica removal for the three pH's was observed. Table 12 demonstrates that the initial pH of the RO concentrate water varied from a low of pH 3 to pH 8.34. Similar to Experiment 3, it was very difficult to control the pH with the addition of HTC doses. Regardless of the initial pH, the final pH value was typically greater than 12. That research showed that even with initial pH's starting between 3 and 9, the final pH resulted in 12 or greater. Sasan et al. (2017) discovered a similar result using HTC at a dose of 2.4 mM or larger. Sasan et al. (2017) attributed the large pH swings to the reconstruction of the HTC as it rehydrates. As the calcined HTC is hydrated, OH^- ions are released into solution and silica is incorporated into the structure of the HTC. Therefore, regardless of initial pH values of the RO concentrate water, when the calcined HTC was rehydrated similar numbers of OH^- ions were released into solution. This may explain why large percent silica removals and high final pH values are observed when using calcined HTC to remove silica.

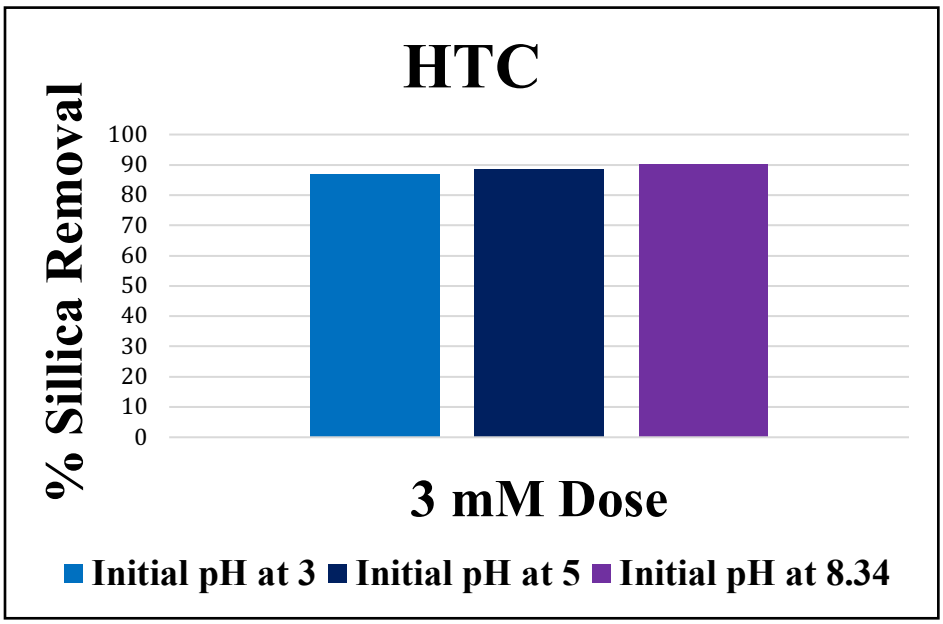

Figure 20: The Percent Silica Removal vs. pH at a 3 mM Dose of HTC.

Discussion of Silica Removal in Experiments 1 through 6

Table 16 presents the PZC for $Mg(OH)_2$, $Fe(OH)_3$ and HTC. According to Table 16, the PZC for the $Mg(OH)_2$ and HTC are 10.8 and 12, respectively. According to the information presented in Chapter 2, the $Mg(OH)_2$ and HTC would have a net positive surface charge because the experimental pH values are all essentially below the PZC. Table 1 presented in Chapter 2 shows the speciation of monomeric silica from pH 7 to pH 14. At pH 9, 13.7% of silica exists as the deprotonated species ($H_3SiO_4^-$). As pH increases, more of the $H_3SiO_4^-$ species exists in solution. The negative charge on the deprotonated $H_3SiO_4^-$ would bind with the positive charge on the absorbent surface. Therefore, larger silica removals were observed using $Mg(OH)_2$ and HTC as the pH increased (Figure 15, 18 and 20). While adsorption mechanisms were considered for by the preformed $Mg(OH)_2$, surface precipitation could be occurring as well.

Material	pH_{pzc}	Reference
$Mg(OH)_2$	10.8	Schott, 1981
$Fe(OH)_3$	8.5	Benjamin, 2002
HTC	12	Han et al., 1981

Table 16: Point of Zero Charge for silica, $Mg(OH)_2$, $Fe(OH)_3$ and HTC.

According to Benjamin (2002), the PZC for $Fe(OH)_3$ is 8.5. Thus, the net surface charge on the $Fe(OH)_3$ would be negative at the tested pH's. However, the surface of the $Fe(OH)_3$ will contain some positive sites which decrease with increasing pH. Therefore, the positive sites are sorbing to the $H_3SiO_4^-$ species which may explain the trends in the data observed in Figure 19. In addition to electrostatic effects, Taylor (1995) proposed that adsorption occurring above the PZC involves direct bonding of the adsorbing sites of the $Fe(OH)_3$ and the silica molecules. The term is called specific adsorption, or inner-sphere complexation, and it is defined as adsorption that is independent of surface charge (Taylor, 1995). While adsorption was investigated for the justification of silica removal by $Fe(OH)_3$, surface precipitation could be occurring as well.

Another suggested theory for the silica removal by the $Fe(OH)_3$ at pH's greater than 8.5 is interparticle bridging. Hunter (2001), describes bridging as polymer chains adsorbing on particle surfaces at the sites of the polymer chain as a result of coulombic interactions, dipole interactions, hydrogen bonding and van der Waals forces of attraction. A hypothesized interparticle bridge reaction was suggested as, at pH > 8.5 the

negative charges on the $Fe(OH)_3$ and $H_3SiO_4^-$ bind with a cation with a 2+ or greater charge forming iron silicate.

Sims (2015) completed a jar test with 2,300 mg/L $Fe(OH)_3$ as Fe^{3+} at a pH ranging from 9.46 – 9.76. To compare the results of Sims (2015) to the research completed for this paper, the Sims (2015) dose was converted to 41 mM $Fe(OH)_3$ by dividing 2,300 mg/L Fe^{3+} by the molecular weight of Fe^{3+} (55.8 mg/mmol) and multiplying by the molar ratio (mmol $Fe(OH)_3$/ mmol Fe^3). By comparison, the most appropriate example for dose and pH used in this research was 30 mM $Fe(OH)_3$ at a final pH 9.92. At a dose of 41 mM, approximately 100% silica removal was achieved and at a dose of 30 mM, 95% silica removal was achieved. These two different results demonstrate that at a dose range of 30 mM to 41mM and pH ranging from 9.46-9.92, approximately 95% silica removal can be achieved.

Design Parameters

The design parameters were determined as a combination of greatest silica removal and molar loading. Based on the results shown on Figures 15 through 20, the HTC at a dose of 3 mM would be ideal for achieving a 90% silica removal. Additionally, the 3 mM dose had the greatest amount of silica loaded onto the solid on a molar basis when compared to $Mg(OH)_2$ and $Fe(OH)_3$. The 3 mM dose was chosen because it can achieve high silica removal with less chemical addition. Significant operational goals for water treatment plants include the optimization of chemicals use and meeting water treatment goals. Both goals are met by selecting these design parameters. The least amount of chemical was desired (3 mM HTC dose) for the maximum amount of silica removal.

While the 3 mM HTC dose was chosen as the best silica removal technology, it does not come without some challenges. For example, large pH swings are common with the HTC. At the doses examined in this work, the pH was essentially uncontrollable, which can be a big problem. For example, operating at pH 12 for HTC could cause the potential for calcium and/or magnesium precipitation depending on the content in the water which would require pH adjustment and the use of additional chemicals.

Other options would be the 30 mM dose of $Fe(OH)_3$ at pH 9 or 100 mM dose of $Mg(OH)_2$ at pH 11. Both of these would provide more than 90% silica removal with a greater amount of pH control. The $Fe(OH)_3$ at lower dose and requires less pH adjustment so it may be preferred as compared to $Mg(OH)_2$.

Isotherm Results

The following experiments were completed to examine the capacity to adsorb for each of the materials and to determine the most applicable adsorption isotherm model (Langmuir or Freundlich). The assumptions for the Langmuir adsorption isotherm are that every adsorption site has the same free-energy change and each site is capable of binding only one adsorbate resulting in a monolayer (Howe et al., 2012). The assumptions for the Freundlich isotherm are that the adsorption sites have different energies and have multilayer adsorption capabilities (Howe et al., 2012).

Experiment 7 examined the relationship of silica adsorbed to $Mg(OH)_2$ at pH 10 and pH 11. Figure 21 displays the mass of silica adsorbed to the $Mg(OH)_2$ (Q_e) vs final aqueous silica concentrations. The adsorbent doses that were tested were 3 mM, 15 mM, 30 mM, 45 mM and 80 mM. At pH 10, the maximum mass loading was 100 mg silica/ g $Mg(OH)_2$ and at pH 11, the final loading was 110 mg silica/ g $Mg(OH)_2$. As the pH

increases, the adsorption capacity increases. The fit of the adsorption data to the Langmuir and Freundlich isotherm models were then tested. The Freundlich isotherm had a better fit due to the linear relationship observed in Figure 22 with an $R^2 = 0.98$ when the values were averaged for pH 10 and pH 11. The Langmuir isotherm (Figure 23) did have a high R^2 value, however, the curves show an exponential growth concave down shape indicating that the Langmuir model did not fit as well. Therefore, it can be assumed that multilayer adsorption occurs in $Mg(OH)_2$.

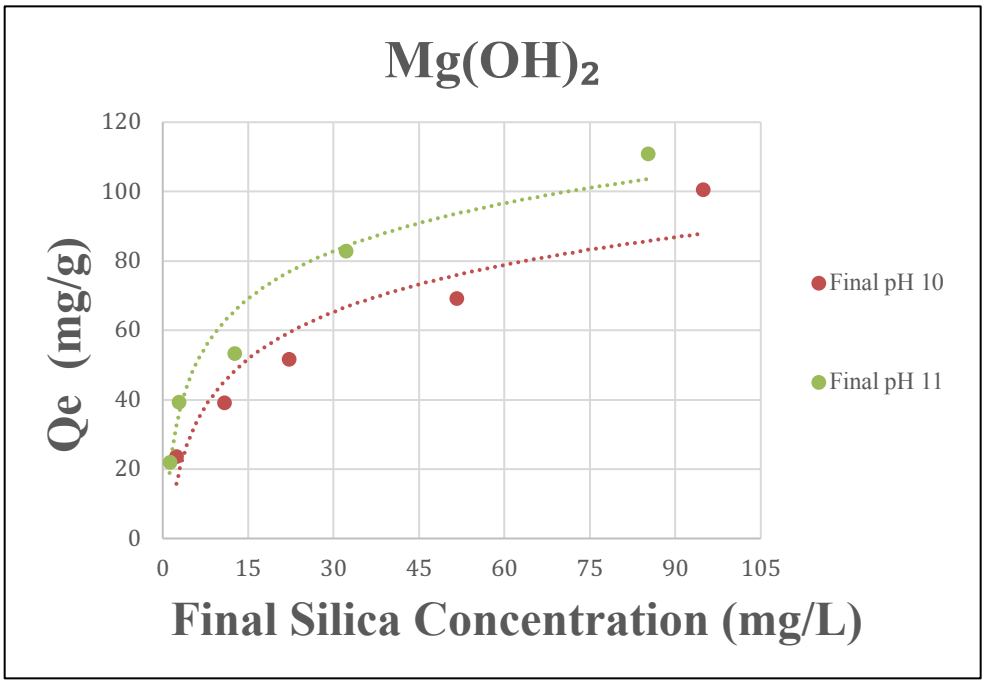

Figure 21: Q_e vs. Final Silica Concentration for $Mg(OH)_2$.

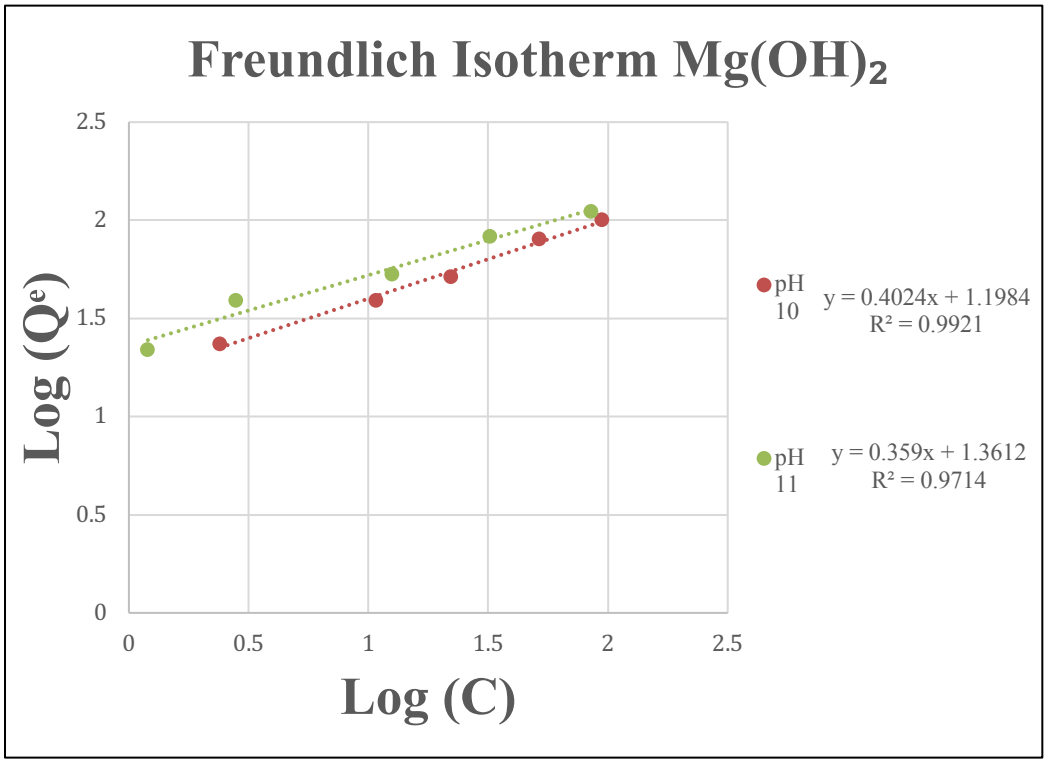

Figure 22: Freundlich Isotherm results for $Mg(OH)_2$.

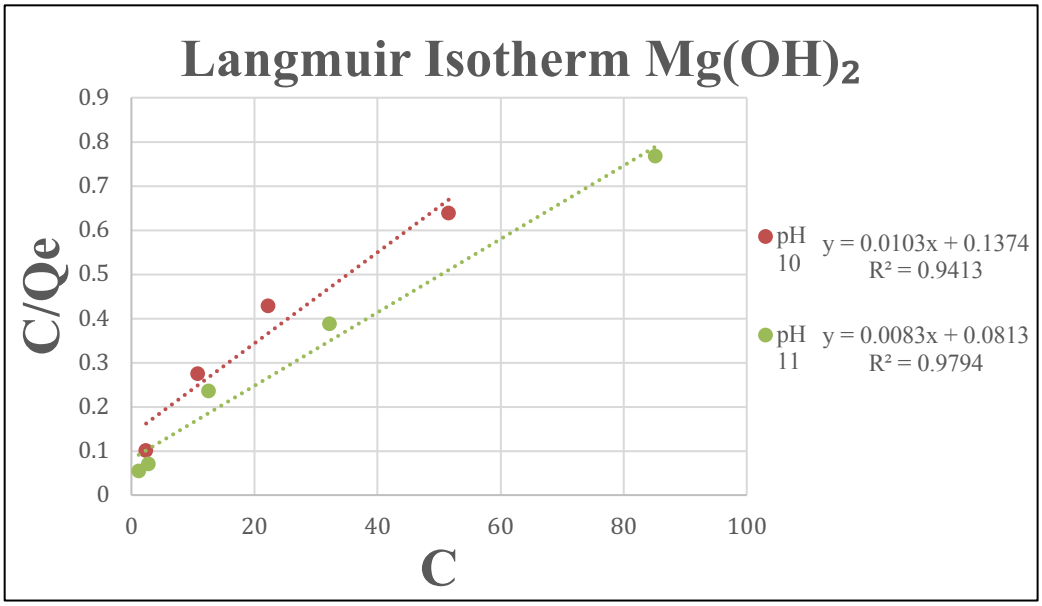

Figure 23: Langmuir Isotherm results for $Mg(OH)_2$.

Experiment 8 examined the adsorption capacity of $Fe(OH)_3$ at pH 9, 9.5 and 10. Figure 24 displays Q_e vs final silica concentrations. The adsorbent doses that were tested were 3 mM, 5 mM, 10 mM, 15 mM and 20 mM. The following final loadings were observed at various pH vales: at pH 9, the final loading was 204 mg silica/ g $Fe(OH)_3$; at pH 9.5, the final loading was 165 mg silica/ g $Fe(OH)_3$; and at pH 10, the maximum mass loading was 132 mg silica/ g $Fe(OH)_3$. As the pH increased, the silica loading on the $Fe(OH)_3$ decreased. In the research completed by Baca (2016), $Fe(OH)_3$ was evaluated to determine the most appropriate model and the best fit was determined to be the Langmuir isotherm model. The Freundlich isotherm model was the most appropriate linear fit with an $R^2 = 0.99$ (Figure 25) for this research and therefore it is assumed to be multilayer adsorption. Huang and Raupach (1967) found that soluble silica has a high affinity for ferric oxides forming multiple layers of sorbed silica. The R^2 values for the Langmuir isotherm (Figure 26) were also high, however, the data points did not form a straight line as compared to the Freundlich isotherm model.

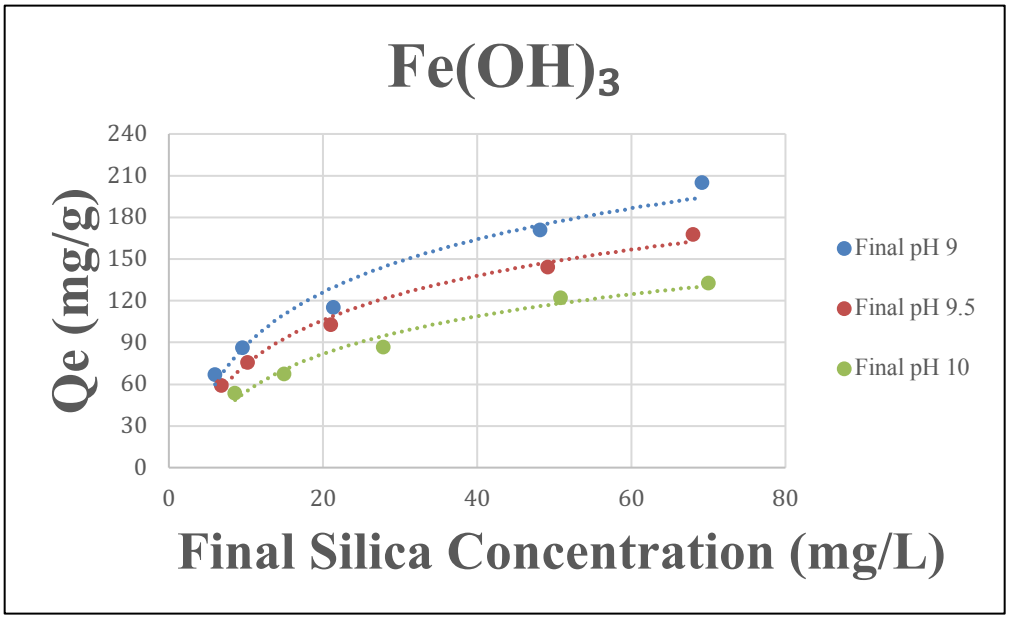

Figure 24: Q_e vs. Final Silica Concentration for $Fe(OH)_3$.

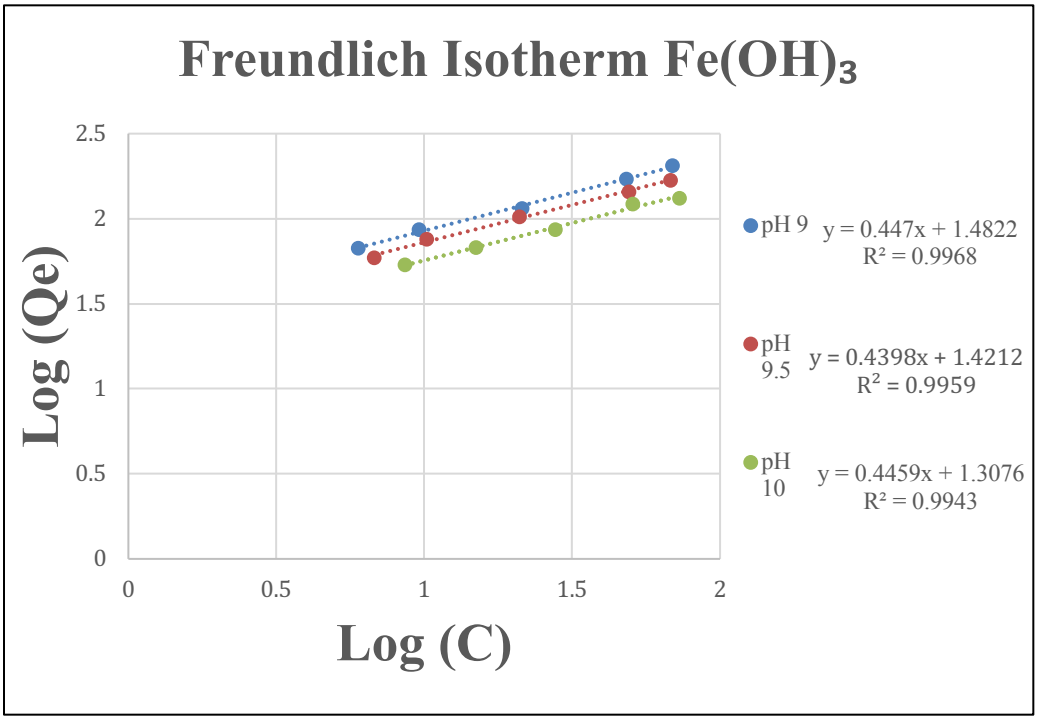

Figure 25: Freundlich Isotherm results for $Fe(OH)_3$.

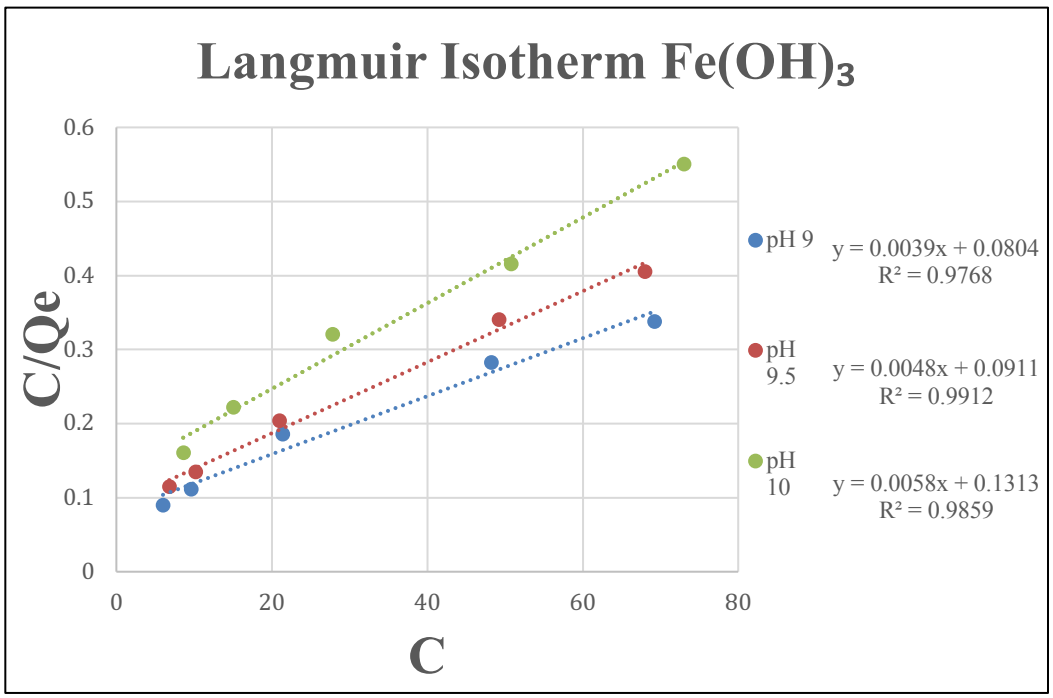

Figure 26: Langmuir Isotherm results for $Fe(OH)_3$.

Experiment 9 examined the adsorption capacity of HTC. Figure 27 displays Q_e vs. final silica concentrations. The doses that were tested were 0.5 mM, 1.5 mM, 2 mM and 2.5 mM. The data on Figure 27 suggests that the loading of silica on the HTC is independent of pH. At the initial pH values of 3, 5 and 8.34 the final loadings were 137 mg silica/g HTC on average. The final pH values were above 11.5. Also, a linear shape was observed, meaning that the HTC has not reached capacity. Using the final loadings formula used in this work ($Q_e = \left(Initial\ Concentration\ \left(\frac{mg}{L}\right) - Final\ Concentration\ \left(\frac{mg}{L}\right)\right)\left(\frac{Volume\ (L)}{Mass\ (g)}\right)$) a calculation was completed to determine the final loading on the HTC from the work completed by Sasan et al. (2017). The parameters used from that work were as follows: initial silica concentration of 50 mg/L; final silica concentration of 25 mg/L; volume of 50 mL; and 10 mg of HTC. The calculated final loading was computed to be 124 mg silica/ g HTC. Using this value, the

final loadings calculated from Sasan et al. (2017) correlated well with the final loadings found in this work. The data on Figure 28 identifies a linear relationship with a $R^2 = 0.90$ for the Freundlich isotherm. Due to the results of this model, it can be assumed that multilayer adsorption of silica occurs in HTC. Figure 29 provides the results of the Langmuir isotherm. The curves observed in Figure 29 are clearly non-linear indicating that this model is not appropriate for this system.

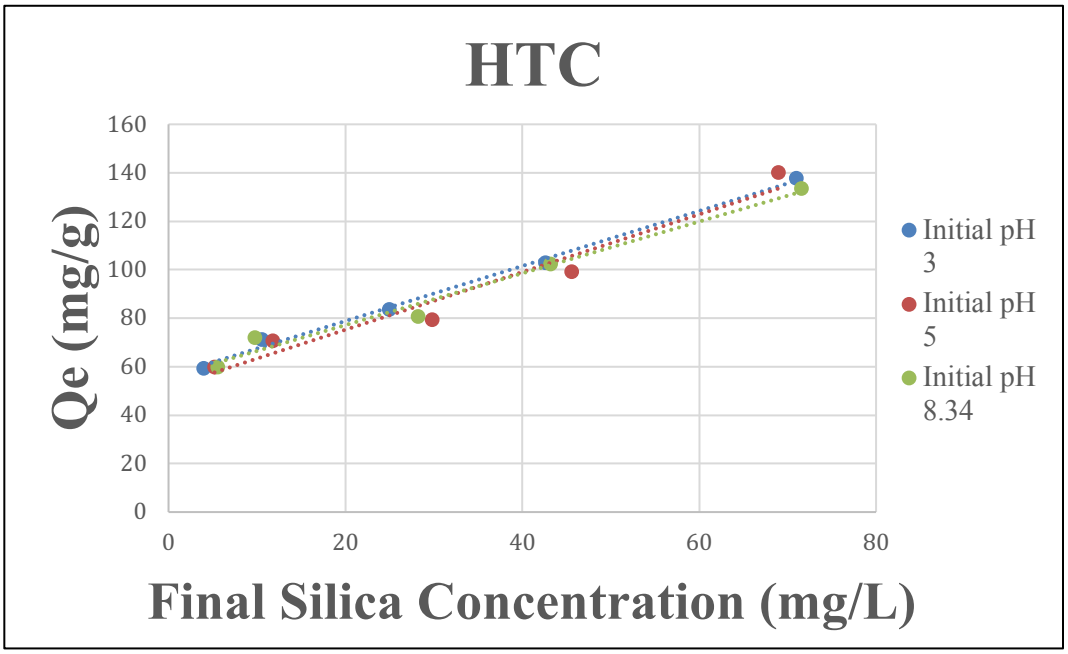

Figure 27: Q_e vs. Final Silica Concentration for HTC.

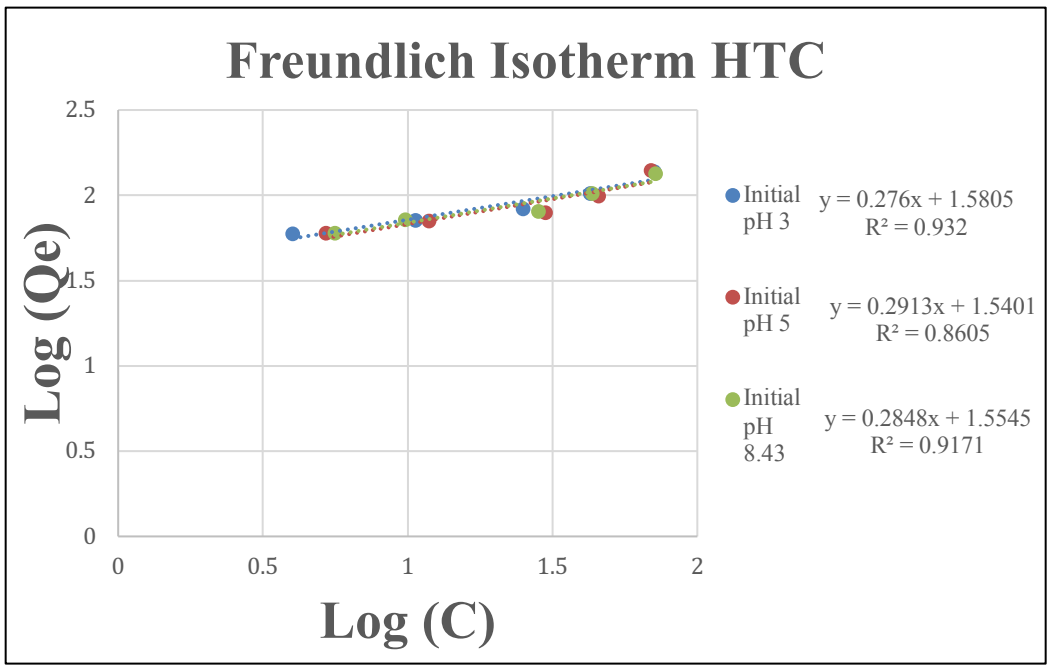

Figure 28: Freundlich Isotherm results for HTC.

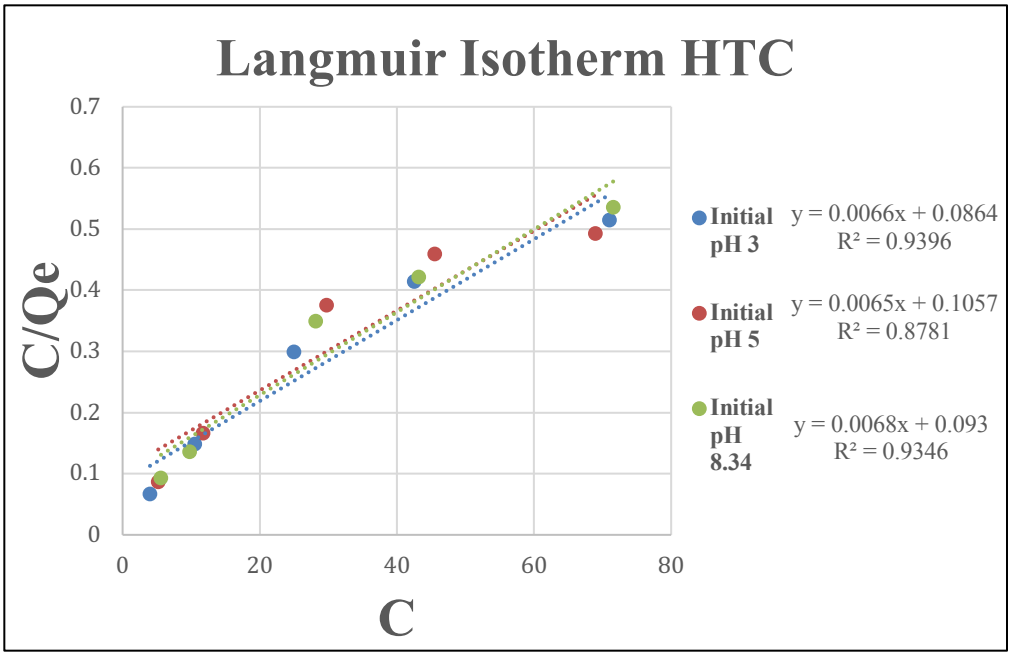

Figure 29: Langmuir Isotherm results for HTC.

Adsorption vs. Surface Precipitation Mechanism for Silica Removal

Stumm and Morgan (1996) created a model to describe the idealized isotherms for ions binding to an oxide. The model represents five relationships: 1. adsorption only; 2. adsorption and surface precipitation; 3. adsorption and heterogeneous nucleation in the absence of free energy nucleation barrier; 4. adsorption and heterogeneous nucleation of a meta-stable precursor; and 5. adsorption and heterogeneous nucleation of a stable precursor. The five relationships are represented by different shapes observed in the model. Figures 21, 24 and 27 were compared to this model created by Stumm and Morgan (1996) to describe how silica is removed by each of the materials. Figures 21 and 24 show a plateauing shape, which according to Stumm and Morgan (1996) represents adsorption of silica onto the preformed $Mg(OH)_2$ and $Fe(OH)_3$. However, the points that correspond to the largest loading of silica in Figures 21 and 24 could potentially be increasing linearly, which would correspond to adsorption and surface precipitation of silica onto the solid. While the ratios of sorbate/sorbent were not large enough to conclude that both adsorption and surface precipitation were occurring, it cannot be ruled out. As shown in Figure 27, the linear relationship was not represented by the Stumm and Morgan (1996) model so no comparison was made.

Freundlich Isotherm Parameters

The Freundlich isotherm parameters obtained from Experiments 7 through 9 are summarized in Table 17. The Freundlich adsorption isotherm is $Q_e = KC^{1/n}$. In a linear form, the equation is $\log(Q_e) = \log(K) + (\frac{1}{n})(\log(C)$ (Howe et al., 2012). Based on the results found in Figure 21, 24 and 27 the parameters determined were slope (1/n, Freundlich adsorption intensity parameter) and y-intercept (K, Freundlich adsorption

capacity). The 1/n values (sorption intensity) were examined for the $Mg(OH)_2$, $Fe(OH)_3$ and HTC. If the value of n = 1 then the line is straight with a slope of K, if the value of n > 1 then the slope of the line exponentially grows concave up, and when the value of n < 1 then the line exponentially grows concave down. All 1/n values were less than one. Table 17 suggests that pH does not affect the adsorption intensity due to the similarity in the 1/n values of the materials. Additionally, when the materials were compared, the largest adsorption intensity for silica onto the solid occurred with $Fe(OH)_3$ and the smallest with HTC.

The K values were compared for $Mg(OH)_2$, $Fe(OH)_3$ and HTC. The largest Freundlich adsorption parameter (K) values occurred with the HTC. As pH values were increased from 10 to 11 for $Mg(OH)_2$, the K values increased which is supported by Figure 21 and Table 19. Finally, when examining the K value demonstrated with the $Fe(OH)_3$ at pH 9, 9.5 and 10, the general trend observed is that increasing pH values corresponds to decreasing K values. This is supported by the data in Figure 19 and Table 17. Using the results of Experiments 7 through 9, the K values can be used for determining the proper dose of chemical adsorbent to add to a system in order to achieve a target removal of silica.

Material	pH	1/n = Slope	Log(K) = Intercept	K
$Mg(OH)_2$	10 11	0.40 0.36	1.20 1.36	15.9 mg/g(L/mg)$^{0.40}$ 22.9 mg/g(L/mg)$^{0.36}$
$Fe(OH)_3$	9 9.5 10	0.45 0.44 0.45	1.48 1.42 1.31	30.8 mg/g(L/mg)$^{0.45}$ 26.3 mg/g(L/mg)$^{0.44}$ 20.3 mg/g(L/mg)$^{0.45}$
HTC	3* 5* 8.34*	0.28 0.29 0.29	1.58 1.54 1.56	38.1 mg/g(L/mg)$^{0.28}$ 34.7 mg/g(L/mg)$^{0.29}$ 35.9 mg/g(L/mg)$^{0.29}$

* Indicates the initial pH values.

Table 17: The Freundlich Isotherm Parameters.

Kinetic Results

In Experiments 10 through 12, the adsorption rate of silica onto each of the materials was examined over a period of 50 minutes. The experiments used the adsorbent doses of 30 mM $Mg(OH)_2$, 15 mM $Fe(OH)_3$ and 1.5 mM HTC, respectively. Different doses of the adsorbent were used due to the rapid adsorption of silica observed using $Fe(OH)_3$ and HTC. The data were fitted to zero, first and second order kinetic models. According to Howe et al. (2012), second order reactions depend on collision between the two molecules of the same species or different species. Figures 30, 31 and 32 depict the results of each of the kinetic models.

The results for the adsorption rate of silica onto the 30 mM dose of $Mg(OH)_2$ appear to be second order kinetics due the linear relationship observed in Figure 32. The R^2 value for this line was 0.9659. The second order kinetic reaction rate constant was 3.0

X 10^{-4} mg/L·min. The zero and first order kinetics did not show a linear relationship for the $Mg(OH)_2$.

The results for the adsorption of silica on the 15 mM dose of $Fe(OH)_3$ were not as definitive as the $Mg(OH)_2$. The strongest linear relationship did occur for second order kinetics, however, the R^2 value was only 0.7505 (Figure 32). The second order kinetic reaction rate constant was 9.0 X 10^{-5} mg/L·min. The first order kinetic model (Figure 31) resulted in an R^2 value of 0.7051 which is less than the R^2 value in the second order kinetics. Therefore, it can then be assumed that the $Fe(OH)_3$ follows a second order kinetics model.

Sasan et al. (2017) demonstrated that the uptake of silica by HTC occurs with pseudo second order kinetics. Sasan et al. (2017) had an R^2 value of 0.99. However, the pseudo second order kinetic model plots time divided by Q_e vs time and was not considered in this work because as time increases Q_e becomes negligible. Therefore, the plot becomes time vs time and it may not adequately represent the uptake of adsorbate. Nevertheless, zero, first and second order kinetics models were studied for the 1.5 mM dose HTC. The HTC showed moderately strong correlations to the second order kinetic model (Figure 32). The R^2 value was 0.89 which was not as strong of a linear relationship as the $Mg(OH)_2$ but was stronger than the $Fe(OH)_3$. Using the slope of the line presented in Figure 32, the reaction rate constant for silica on HTC was 7.0 X 10^{-5} mg/L·min.

The rate constants followed the second order kinetics model and were determined to be 3.0 X 10^{-4} mg/L·min for $Mg(OH)_2$, 9.0 X 10^{-5} mg/L·min for $Fe(OH)_3$ and 7.0 X 10^{-5} mg/L·min for HTC. Therefore, for every minute 3.0 X 10^{-4} mg/L of silica is adsorbed to

$Mg(OH)_2$, 9.0 X 10^{-5} mg/L of silica is adsorbed to $Fe(OH)_3$ and 7.0 X 10^{-5} mg/L of silica is adsorbed to HTC. Additionally, the uptake rates were calculated on a molar basis and were determined to be 5.14 X 10^{-6} mmol/L·min for $Mg(OH)_2$, 8.42 X 10^{-7} mmol/L·min for $Fe(OH)_3$ and 1.16 X 10^{-7} mmol/L·min for HTC.

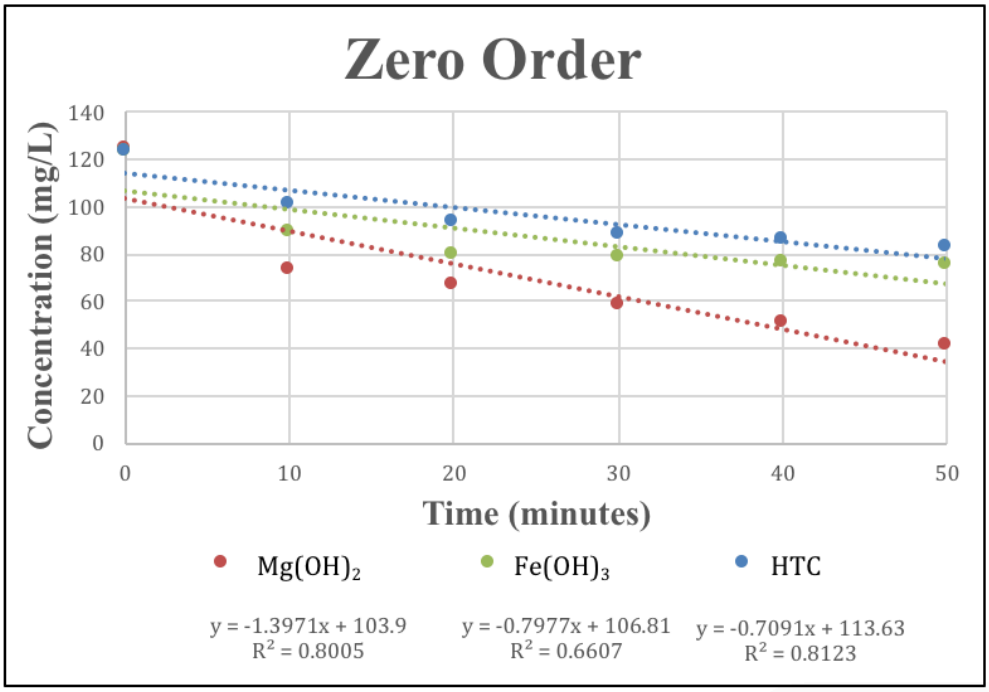

Figure 30: Zero Order Kinetic results.

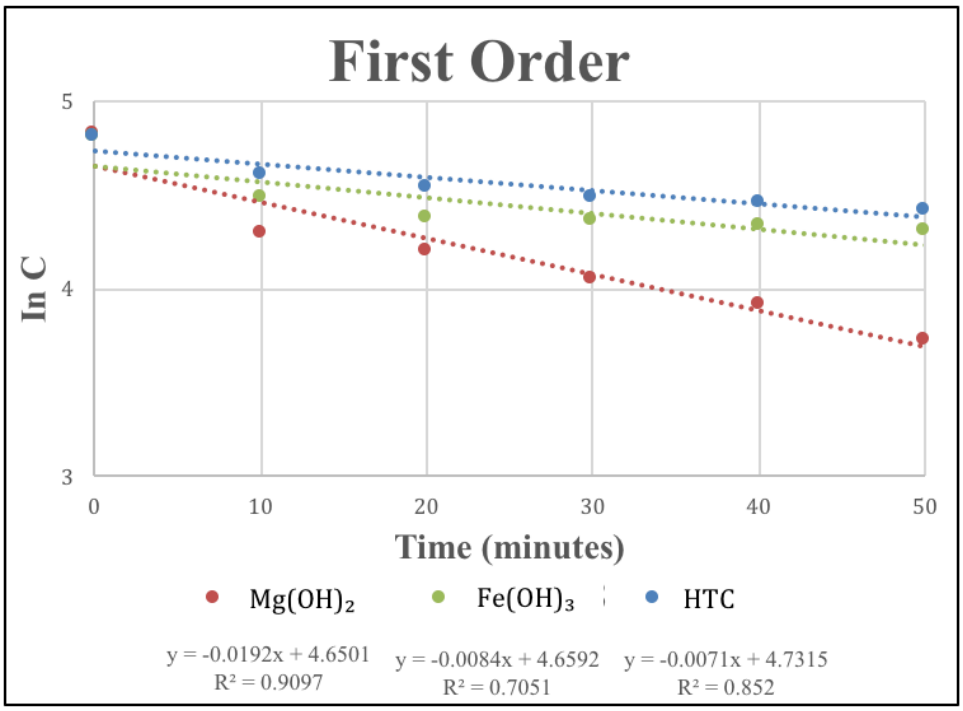

Figure 31: First Order Kinetic results.

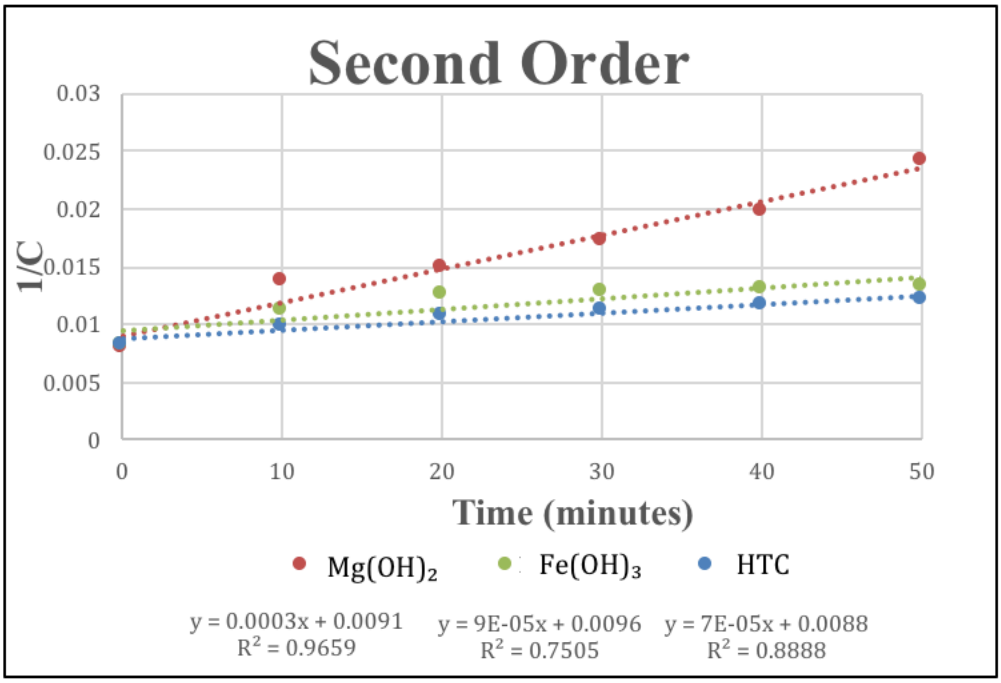

Figure 32: Second Order Kinetic results.

Implications of Rate Constants

The rate constants indicate the speed of the reaction of silica onto the solids. If a final target percent silica removal is desired, the rate constants can be used in a mass balance to determine the volume of a theoretical reactor. The mass balance equation can be summarized by $[accum] = [mass\ in] - [mass\ out] + [rxn]$, where [accum] = 0 (steady state), [mass in] or [mass out] = QC (flow times silica concentration) and [rxn] = Vr (volume times rate constant) (Howe et al., 2012) (Figure 33). If the rate constants, flows and the target silica removal were known, then the mass balance could be rearranged so final volume of the reactor could be determined to achieve the target silica removal.

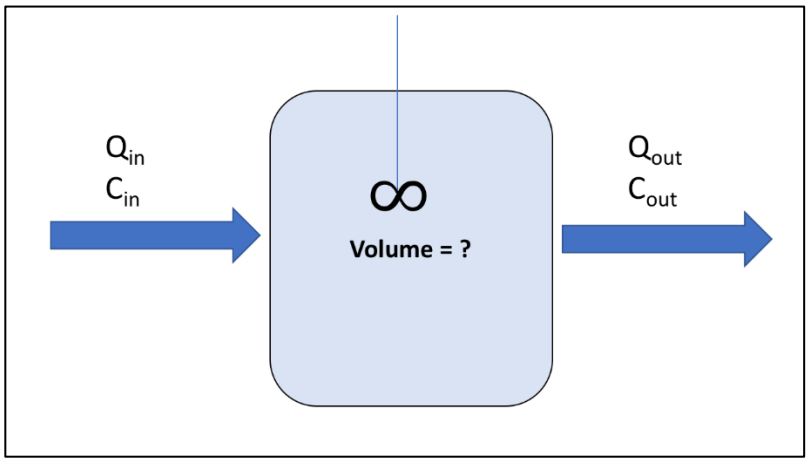

Figure 33: A theoretical CMFR used for the mass balance calculations.

Silica Removal Mechanism by HTC

HTC has been shown to remove silica, but the mechanism has yet to be well documented. This purpose of this section is to develop a hypothesis for a removal mechanism examining existing literature and then using experimental results to attempt

to confirm the hypothesis. The overall molecular formula of HTC was described by Bontchev et al. (2003):

$$\left[M_{1-x}^{(II)}\, M_x^{(III)}(OH)_2\right]^{x+}[A]_x^- \cdot mH_2O$$

where $M^{(II)}$ = Ca^{2+}, Mg^{2+}, Mn^{2+}, Fe^{2+}, Co^{2+}, Ni^{2+}, Zn^{2+}; $M^{(III)}$= Al^{3+}, Cr^{3+}, Mn^{3+}, Fe^{3+}, Co^{3+}, Ga^{3+}; A = Cl^-, Br^-, I^-, NO_3^-, CO_3^{2-}, SO_4^{2-}, silicate, polyoxometalate and/or organic anions. For this work, Mg^{2+} was used as $M^{(II)}$, Al^{3+} was used as $M^{(III)}$ and CO_3^- was used as A. The HTC structure contains alternating Mg^{2+} and Al^{3+} ions surrounded by six hydroxyl groups in an octahedral co-ordination that share edges forming infinite sheets (Baskaran et al., 2015). When hydrated the infinite sheets are stacked forming a layered network held together by hydrogen bonds (Baskaran et al., 2015). Due to the presence of Al^{3+} anion, the electrical neutrality in the interlayer positions is maintained by the anion CO_3^{2-} and water (Constantino and Pinnavaia, 1995). But, these anions and water molecules in the interlayers of the HTC can be replaced by various organic and inorganic anions including silicates (Baskaran et al., 2015). Baskaran et al. (2015), stated that silicate anions were introduced to the layers of the HTC which act as pillars and were expected to increase porosity and thermal stability. The basic structure of silicates can be best described as four oxygen molecules covalently bound to one silicon molecule (SiO_4^{4-}) forming a tetrahedron. Based on this literature, it appears the HTC incorporates silica into its structure when rehydrated.

To test this hypothesis, an experiment was conducted with Hach Silica Standard and DI water to avoid the ions and alkalinity in the RO concentrate water. The goal of this experiment was to perform a mass balance to compare silica uptake to hydroxyl groups released. Table 18 displays the pH and concentrations of silica throughout the

time period that the test was completed. The amount of silica bound on the HTC and the release of hydroxyl groups were calculated. The last column in Table 18 shows a ratio of bound silica onto HTC per released hydroxyl group. In the first five minutes 102 moles of silica was bound per one mole of hydroxyl group. Over time, the moles silica bound to HTC decreases, however, the ratio is high (40:1). When the layers of Mg^{2+} and Al^{3+} become hydrated with the Hach Silica Standard diluted with DI water, the interlayers of the HTC are reformed with silica and water molecules. Over time, the percent silica removal increased as well as the pH. The pH increase is due to the release of hydroxyl groups as the silica binds to the Mg^{2+} and Al^{3+} octahedral. This forms a sandwich between the two infinite sheets of Mg^{2+} and Al^{3+}. As time increases, the pH increase will plateau resulting in the adsorption capacity being reached.

Time (min)	pH	pOH	Silica Concentration (mg/L)	Silica Bound on HTC (moles)	Hydroxyl Groups Released from HTC (moles)	Ratio Silica: Hydroxyl
0	8.13	5.87	132	0	0	0
5	8.64	5.36	113.6	1.53×10^{-4}	1.51×10^{-6}	102
15	8.93	5.07	109.4	1.88×10^{-4}	3.58×10^{-6}	53
30	9.07	4.93	104	2.33×10^{-4}	5.20×10^{-6}	49
60	9.14	4.86	101.8	2.51×10^{-4}	6.23×10^{-6}	40

Table 18: The calculations for how many moles of silica were bound to HTC per release of hydroxyl groups.

Table 19 presents the results of an analogous experiment completed with RO concentrate water. This experiment was completed with a different water source to compare the silica uptake with the ions found in the RO concentrate water. It appears with the additional buffering of the solution the number of bound moles of silica and pH

decrease in the first five minutes. The data suggests that the number is nearly cut in half. However, as time progresses the numbers become similar to the previous experiment. While, the ions may inhibit some of the silica from binding to the HTC, the results still show a high number. This data indicates that silica uptake per hydroxyl group are related, however, the exact mechanism was not determined. Additional work should be completed to determine the exact mechanism in which HTC uptakes silica.

Time (min)	pH	pOH	Silica Concentration (mg/L)	Silica Bound on HTC (moles)	Hydroxyl Groups Released from HTC (moles)	Ratio Silica: Hydroxyl
0	7.89	6.11	121	0	0	0
5	8.83	5.17	103	1.50×10^{-4}	3.00×10^{-6}	51
15	9.11	4.9	94.6	2.20×10^{-4}	6.05×10^{-6}	35
30	9.25	4.75	86.4	2.88×10^{-4}	8.50×10^{-6}	33
60	9.38	4.63	79.4	3.46×10^{-4}	1.16×10^{-5}	30

Table 19: The calculations for how many moles of silica were bound to HTC per release of hydroxyl groups in the RO concentrate water.

Continuous Membrane Filtration Experiments

Sims (2015) found that a single dose of $Mg(OH)_2$ and $Fe(OH)_3$ could be introduced to a similarly designed flow-through system as the one used for this paper to remove silica. This work expanded the work of Sims (2015) by adding fresh doses of adsorbent at 1-hour intervals to achieve a desired silica removal. Experiments 13 through 15 used the information gathered in the batch tests to determine parameters such as absorbent dose and pH for the freshly precipitated $Mg(OH)_2$, freshly precipitated $Fe(OH)_3$ and calcined HTC. Additionally, Sims (2015) found a similar result of rapid uptake of silica onto the solids ($Mg(OH)_2$ and $Fe(OH)_3$) and used a HRT of 20 minutes

with a similarly constructed system. In order to be consistent with and allow for comparison to the work done by Sims (2015) and considering the rapid uptake of silica, a Q of 110 mL/min was selected and the resulting HRT was determined to be 24.5 minutes.

A silica removal efficiency of 70% was the figure determined for the selection of the design parameters which also allowed for comparison with previous work by Sims (2015). The pH values selected were determined from Experiments 4 through 6 as follows: pH 11 for $Mg(OH)_2$; pH 9 for $Fe(OH)_3$; and pH > 9 for HTC. The dose for each of the materials were determined by the results of Experiments 7 through 9. For example, in Figure 21 at approximately 37 mg/L (70% silica removal) a vertical line was traced until the pH 11 line was intersected. At the point where the vertical line intersects pH 11, a horizontal line was traced to the y-axis to determine a loading (Q_e) of 85 mg/g. A dose calculator was created to determine the proper amount of chemical to add. The dose calculator uses the removed silica and divides it by the target loading. For example, with an initial silica concentration of 124 mg/L, 87.5 mg/L would be removed and divided by the loading 85 mg/g to get a dose 1.03 g/L of $Mg(OH)_2$ or approximately 19 mM. Analogous computations were computed for the $Fe(OH)_3$ and HTC. The $Fe(OH)_3$ at a desired pH value of 9.0 and dose of 7 mM and the HTC had a desired pH value of >9 and dose 1.4 mM. A summary of the desired parameters can be seen in Table 20.

Material	Desired removal (%)	Desired Density (mg/g)	Target Dose (mM)	Desired pH
Experiment 10 $Mg(OH)_2$	70	85	19	11
Experiment 11 $Fe(OH)_3$	70	120	7	9.5
Experiment 12 HTC	70	100	1.4	> 9

Table 20: A summary of parameters used in each experiment.

Experiment 13

Experiment 13 was completed between the pH values 10 and 11.02 and at an HRT of 24.5 minutes. Figure 34 identifies the results. The 19 mM dose of $Mg(OH)_2$ was introduced every hour to attempt to reach a 70% removal goal. Every hour a new dose was added to the system and allowed to mix for 15 minutes prior to taking a sample. The lowest percent removal occurred at the initial dose and was determined to be attributed to the low initial pH. As the experiment progressed, the pH stabilized, and the 70% removal goal was achieved. The range of silica removal was from 52% to the maximum amount of 70% which occurred in the fourth hour of this experiment. This experiment proved that approximately 70% silica removal could be achieved over a period of 5 hours.

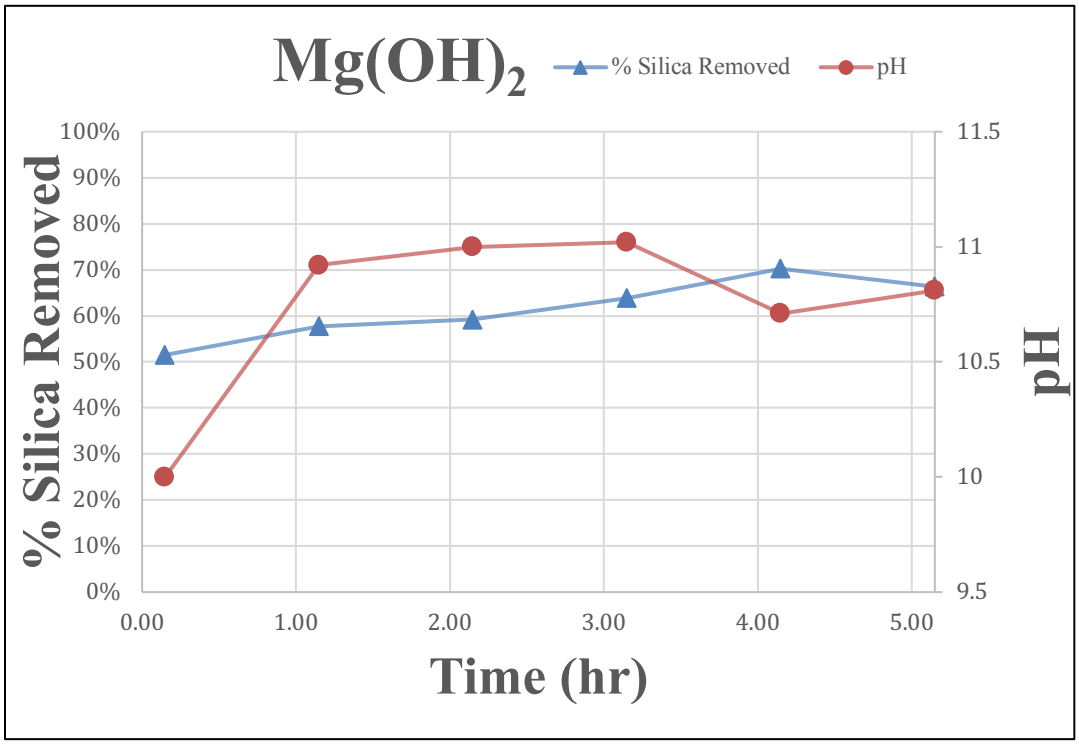

Figure 34: Flow Through Experimentation Using New $Mg(OH)_2$ Every Hour.

Experiment 14

Experiment 14 was conducted using a dose of 7 mM $Fe(OH)_3$ and a pH of 9.5. Due to membrane fouling, the flowrate was lower than the desired calculations resulting in the dose of $Fe(OH)_3$ fluctuating between 7 mM and 9 mM and the HRT increased from 31 minutes to 34 minutes. The pH varied between 8.36 and 10. The percent removal of silica was between 45% and 68%. The initial dose had the lowest removal and the target percent removal was not reached until the fifth hour. However, Figure 34 demonstrates that a percent removal could be maintained. Sims (2015) completed a flow through test at pH 10 with a $Fe(OH)_3$ concentration of 2.3 g/L as Fe^{3+}. To compare the doses on a molar basis the 2.3 g/L as Fe^{3+} was converted to 41 mM $Fe(OH)_3$. At the pH value and dose, Sims (2015) found approximately 12% removal of silica in 0.5 hours. The largest silica removal occurred at 1.5 hours with approximately 80% and silica removal decreased with time. Comparing the results of Sims (2015) to Experiment 14, a significantly smaller dose was used in Experiment 14 to achieve a peak removal of 68% and an overall average of about 60% silica removal across 5 hours. However, the total dose of $Fe(OH)_3$ added to the system was similar to Experiment 14, having a total $Fe(OH)_3$ dose of approximately 40 mM. When the average percent silica removals were compared across each of the experiments, similar percent removals were observed with Sims (2015) achieving an average silica removal of 57% and Experiment 14 achieving 60% removal. Overall, Experiment 14 was successful because a steady percent removal was achieved in 5 hours.

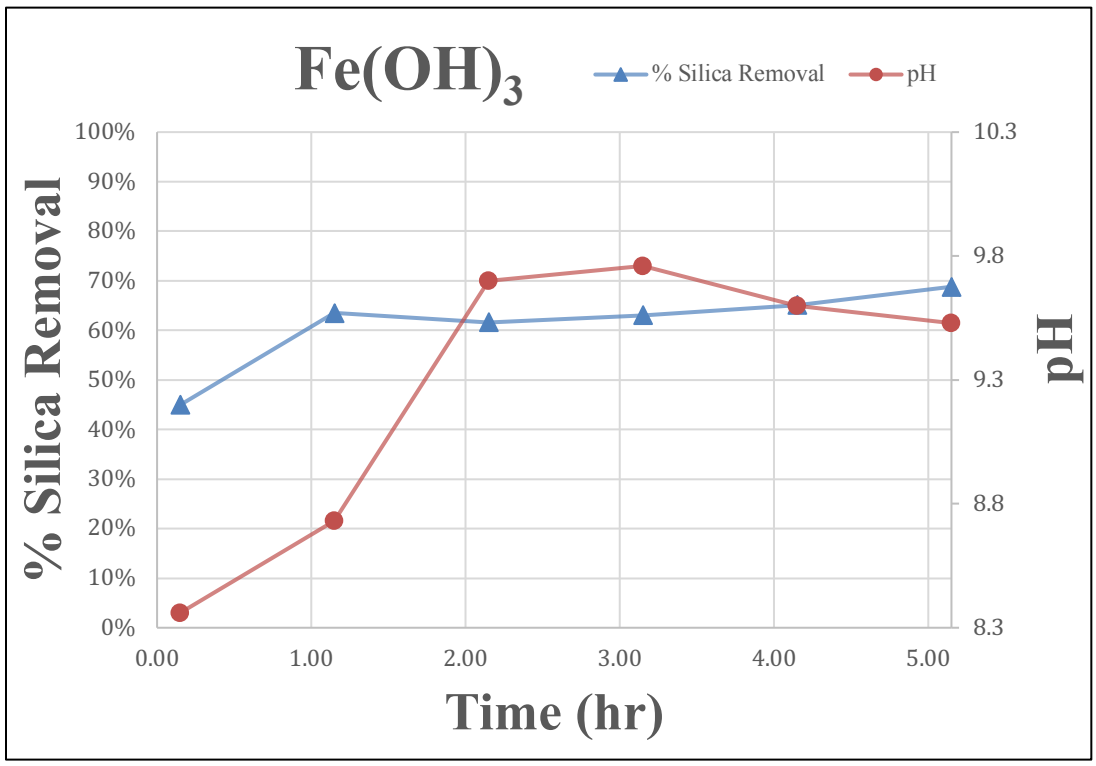

Figure 35: Flow Through Experimentation Using New $Fe(OH)_3$ Doses Every Hour.

Experiment 15

Sims (2015) showed that freshly precipitated $Mg(OH)_2$ and freshly precipitated $Fe(OH)_3$ could be introduced to a flow through system at a single dose to achieve the removal of silica. HTC was not considered for Sims (2015) work. Before the HTC was introduced continuously to achieve a target percent removal, different single doses of HTC were introduced to the flow through system. Figure 36 displays the single dose results. Each dose was loaded into the system and the system was then closed and ran for 3 hours. At a dose of 0.37 g/L of HTC, the greatest percent silica removal occurred at 0.5 hour and was 68%. As time progressed through the experiment, fresh RO concentrate water (124 mg/L silica) entered the system and the HTC continued to adsorb the silica until the material reached its capacity. The percent removal decreased over time due to

the capacity of the HTC being reached. At a dose of 0.74 g/L HTC, the greatest percent silica removal occurred 85% and at a dose of 1.11 g/L HTC the percent removal was 91%. Similar to Sims (2015), these tests confirm that HTC is a viable material for the flow-through system.

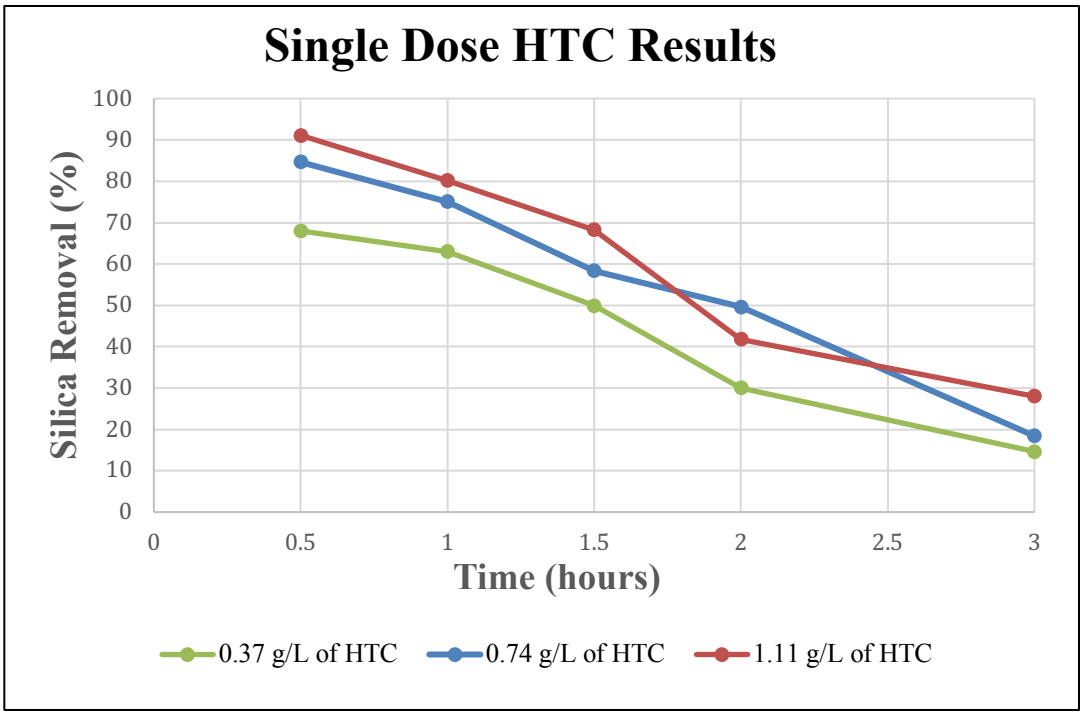

Figure 36: Flow Through Experimentation with Single Dose of HTC.

Experiment 15 was completed by dosing with fresh HTC every hour. The pH varied between 9.21 and 9.9 and doses varied from 1.4 mM to 2.2 mM due to membrane fouling. Because of low flow through the membrane the HRT varied from 42 minutes to 44 minutes. While, the target HRT was 24.5 min, altering the HRT did not show a decrease in silica removal. The greatest percent removal was 74% and the average percent removal for the second dosing through the fifth dosing was about 66%. The results are summarized in Figure 37. The results indicate that a 70% silica removal could be achieved with a varying dose of 1.4 mM to 2.2 mM at pH >9.

Some interesting findings were observed when comparing the batch studies and flow through studies using the HTC. The batch studies presented difficulties in controlling the pH while in Experiment 12 the pH did not increase above 11. The difference in the results was determined to be a variance in experimental configurations. The batch study had a set volume of RO concentrate water with a silica concentration of 124 mg/L in a centrifuge tube. The HTC was introduced and allowed to mix for an allotted amount of time. The results showed high silica removals and high pH values, but the continuous flow experiments involved continuous feed of the RO concentrate with periodic addition of HTC. HTC was introduced to the system and silica concentrations decreased initially, and pH increased due to the release of OH^- groups. As time increased, the silica concentration and pH in the system stabilized because of the pumping of the new RO concentrate water into the system. The pH increased following addition of the HTC then declined until its next addition.

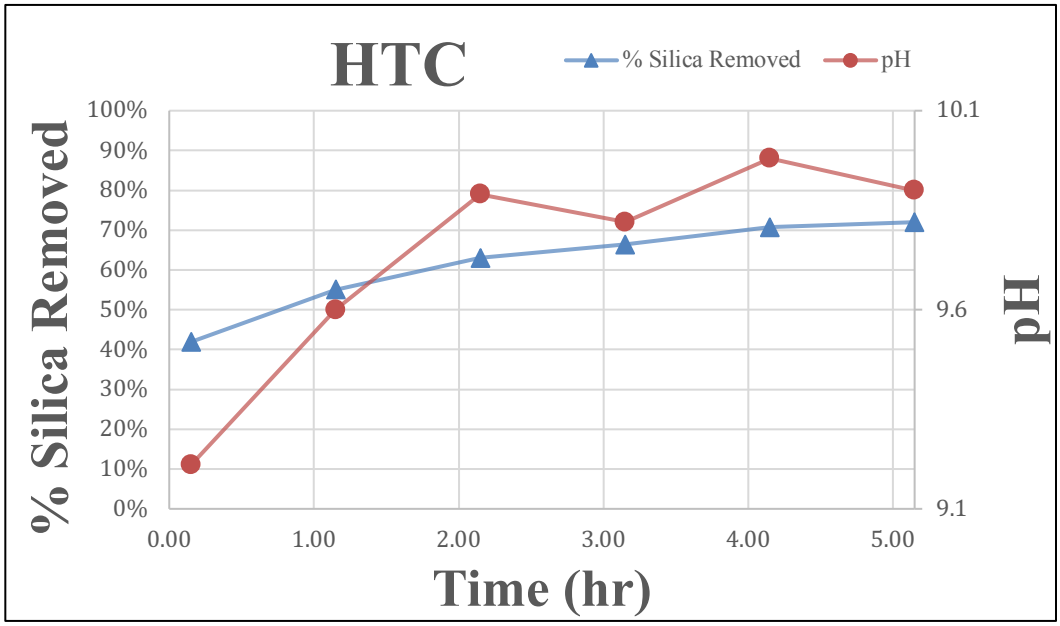

Figure 37: Flow Through Experimentation Using New HTC Doses Every Hour.

Membrane Fouling

Sims (2015) used a 1% citric acid solution to clean and restore the membrane to the initial flow for her flow through experiments. This work did not use membrane cleaning to restore the flowrate. The initial flow of 110 mL/min was only achieved in Experiment 13. Over time, the flow decreased and in the last measurement the flow was 103 mL/min. Similarly, the $Fe(OH)_3$ permeate flow began at 85 mL/min and steadily declined to 78 mL/min and the HTC flow began at 63 mL/min and declined to 61 mL/min. The decrease in permeate flow was attributed to membrane fouling. Flux was used to determine if the reduction if flow rates was due to membrane fouling. Flux is defined as permeate flow per membrane area. Flux is defined as permeate flow per membrane area as shown in Equation 15.

$$\text{Flux} = \frac{Permeate\ Flow\ (\frac{L}{hr})}{Membrane\ Area\ (m^2)} \quad (15)$$

The permeate flow was measured using a graduated cylinder and stopwatch and the POREX® membrane area was 0.069 m^2. Figure 38 demonstrates the loss in flux across Experiments 13 through 15. The three materials showed comparable trends of decreasing flux. The percent loss was calculated to determine the loss of flux for each of the materials. Percent losses were determined by the change in flux presented in Figure 38. The $Mg(OH)_2$ had an 6.3% loss, the $Fe(OH)_3$ had an 8.2% loss and the HTC had an 1.6% loss.

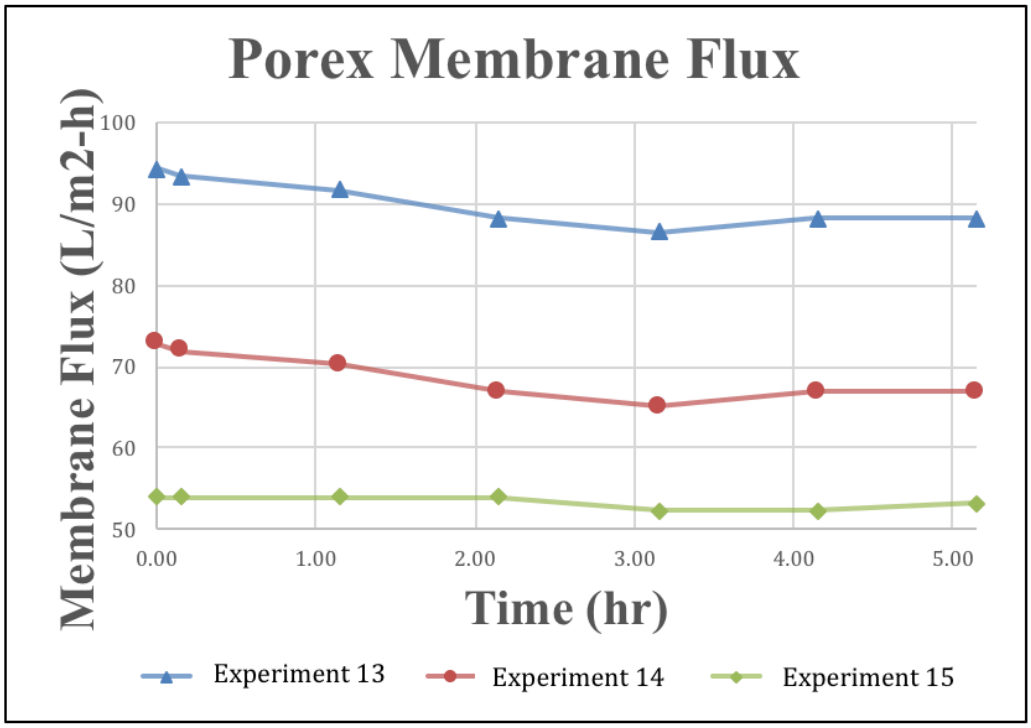

Figure 38: The Membrane Flux vs. Time in Experiments 13 Through 15.

In addition to flux, specific flux was also determined using Equation 16.

$$(16)\quad Specific\ Flux = \frac{Flux\ (\frac{L}{m^2-h})}{Delta\ Pressure\ (bar)}$$

The percent loss of Specific Flux also was calculated for each of the materials. The $Mg(OH)_2$ had a loss of 40.1%, the $Fe(OH)_3$ had a loss of 47.6% and the HTC had a loss of 51%. HTC had the largest loss with 51% although all of the materials showed losses above 40%. The results of the percent loss calculations through Flux and Specific Flux prove that membrane fouling did occur in Experiments 13 through 15. However, similar to Sims (2015) the decline in the flux did not result in a decrease in percent silica removal.

CHAPTER 5: CONCLUSION

Silica is found in almost all-natural waters and is considered a contaminant because it can polymerize forming scale on industrial equipment and RO membranes at high concentrations. The removal of silica is particularly challenging due to the multiple silica species existing at various concentrations, temperatures and pH values. Successful soluble silica removal from water was demonstrated by Sims (2015), Baca (2017) and Sasan et al. (2017) using various materials and experimental techniques and designs. While their research did have significant findings, there was no comparison of freshly precipitated $Mg(OH)_2$, freshly precipitated $Fe(OH)_3$ and calcined HTC in the overall effectiveness of silica removal. The goal of this research was to directly compare freshly precipitated $Mg(OH)_2$, freshly precipitated $Fe(OH)_3$ and calcined HTC by altering the design parameters (dose and pH) and examining how these variations affect the silica removal process.

To accomplish this goal, 6 major objectives were determined. The objectives for this work were: (1) Investigate and compare the doses of the $Mg(OH)_2$, $Fe(OH)_3$ and HTC required to achieve similar removal efficiency for silica; (2) Investigate the effect of pH on silica removal using $Mg(OH)_2$, $Fe(OH)_3$ and HTC; (3) Investigate and compare the sorption density of silica on $Mg(OH)_2$, $Fe(OH)_3$ and HTC at equilibrium to determine the most applicable adsorption isotherm (Freundlich or Langmuir), and identify isotherm parameters; (4) Investigate and compare the kinetics of silica sorption onto $Mg(OH)_2$, $Fe(OH)_3$ and HTC; (5) propose a mechanism for how HTC removes silica; and (6) Determine design parameters (dosing, pH and HRT) for the flow through system. To

accomplish these objectives, experiments were completed using batch and flow through configurations.

Experiments 1 through 3 examined the effect of molar dose of $Mg(OH)_2$, $Fe(OH)_3$ and HTC on silica removal at pH 10. At a dose of 3 mM, HTC achieved approximately 90% silica removal. At the same molar dose, $Mg(OH)_2$ and $Fe(OH)_3$ removed approximately 15% and 35%, respectively. The general trend observed in the data was an increase molar dose led to an increase in silica removal. However, when the molar doses were compared using the final silica loadings (Q_e (mg/g)) an opposite trend was observed of increased molar dose to decreased final loading. At a dose of 3 mM, $Fe(OH)_3$ had the largest final loading of approximately 146 mg/g. At the same dose, HTC had the lowest final loading with 54 mg/g. Overall, the results of Experiments 1 through 3 identify that a 3 mM dose of HTC had the largest percent removal and the 3 mM $Fe(OH)_3$ had the largest silica loading. This was an important finding because it highlights one important issue when evaluating various adsorption options to remove silica from water. One goal was to achieve a target percent removal attempting to use the smallest dose of chemical adsorbent (i.e. 3 mM HTC dose used in Experiment 3). Another goal would be to attempt to utilize all of the available adsorbent sites or exhaust the adsorbent material to achieve a higher final loading on the solid (i.e. 3 mM $Fe(OH)_3$ dose used in Experiment 2).

Experiments 4 through 6 examined the effect of pH on silica removal. As the pH was increased from 9 to 11, the 3 mM dose of $Mg(OH)_2$ sorbed more silica. An opposite trend was observed in silica removal by the $Fe(OH)_3$ when the pH was increased from 9 to 11. No trends were observed in the final pH values for silica removal using HTC. It

was discovered that at initial pH values as low as 3, the final pH values were mostly all above 12. Therefore, using a 3 mM dose of HTC resulted in approximately 100% silica removal, regardless of initial pH. The mechanism by which the three materials remove silica was examined, and while adsorption mechanisms were considered, surface precipitation cannot be disregarded.

Experiments 7 through 9, tested the sorption density of silica on $Mg(OH)_2$, $Fe(OH)_3$ and HTC at equilibrium to determine the most applicable adsorption isotherm (Freundlich or Langmuir) and identify isotherm parameters. The data for all three materials fit the Freundlich isotherm model as compared to the Langmuir model. This suggests that the materials are capable of multilayer adsorption and that the adsorption sites have different energies. Using the shape of the isotherm graphs, it was confirmed that adsorption was occurring between $Mg(OH)_2$ and silica, and between $Fe(OH)_3$ and silica. However, surface precipitation might be occurring as well. The Freundlich isotherm parameters were determined and are shown in Table 17. The average Freundlich adsorption intensities (1/n) were 0.38 for $Mg(OH)_2$, 0.44 for $Fe(OH)_3$ and 0.29 for HTC. The average Freundlich adsorption capacities (K) were 19.38 (mg/g)(L/mg) for $Mg(OH)_2$, 25.8 (mg/g)(L/mg) for $Fe(OH)_3$ and 36.20 (mg/g)(L/mg) for HTC. Comparing the data above, HTC had the largest adsorption capacity for silica.

Experiments 10 through 12 compared the sorption kinetics onto $Mg(OH)_2$, $Fe(OH)_3$ and HTC. The three materials were examined for zero, first and second order kinetic models. All three materials showed the strongest linear relationships with the second order kinetic models (Figure 32). The uptake rate onto the solids were determined to be 3.0×10^{-4} mg/L·min for $Mg(OH)_2$, 9.0×10^{-5} mg/L·min for $Fe(OH)_3$

and 7.0 X 10^{-5} mg/L·min for HTC. Additionally, the uptake rates were calculated on a molar basis and were determined to be 5.14 X 10^{-6} mmol/L·min for $Mg(OH)_2$, 8.42 X 10^{-7} mmol/L·min for $Fe(OH)_3$ and 1.16 X 10^{-7} mmol/L·min for HTC.

After reviewing literature, a mechanism was proposed for how HTC removes silica. After reviewing the literature, it appears that silica is incorporated into the structure of the HTC as hydroxyl groups are released. To prove this hypothesis, both Hach Silica Standard diluted in DI water (initial silica concentration 132 mg/L) and RO concentrate water (initial silica concentration 121 mg/L) sources were examined using batch test configurations. A ratio was calculated that compared the number of moles of silica bound by the HTC to hydroxyl groups released into the water over time. Both experiments indicated that silica uptakes per hydroxyl group release are rapid and high. The experiment conducted with the RO concentrate water showed a smaller ratio due to the alkalinity of the water. While it was determined that the moles of silica bound per hydroxyl group released was important, no conclusions could be made on the exact mechanism that HTC removes silica.

Experiment 13 to 15 examined if an adsorbent dose could be added to a flow through system once per hour to achieve a target percent removal. These experiments used the results of the Batch Tests to set up the conditions for the flow through tests. Refer to Chapter 4 on how the parameters were selected. One key finding of Experiments 13 through 15 is that 70% silica removal can be achieved with the smallest molar dose using HTC. The 19 mM dose of $Mg(OH)_2$ obtained a 52% to 70% percent removal at an average HRT of 24.5 minutes. The $Fe(OH)_3$ obtained 45% to 68% removal and the HTC was between 66% and 72% with average HRTs of 33.8 minutes and 43.4

minutes, respectively. Due to membrane fouling, doses of $Fe(OH)_3$ and HTC were altered in the respective experiments. The $Fe(OH)_3$ dose fluctuated between 7 mM and 9 mM and the HTC dose fluctuated between 1.4 mM to 2.2 mM. The conclusions of these experiments were that using the results of the Batch Tests, a 70% silica removal could be maintained for 6 hours with all three materials. Although membrane fouling was observed in Experiments 14 and 15 which affected the chemical dose and HRT, the change in flux did not result in decreased silica removal.

Many important findings were discovered during this study. However, there is room for additional work and research on the objectives in this thesis. For example, additional work could be completed on the HTC through SEM, BET and XRD analysis to further analyze a mechanism for how HTC removes silica. Additionally, a study could be completed on gross comparison of material cost. Material costs were obtained from Sigma-Aldrich and MolPort as follows: \$113 per kg for $Mg(OH)_2$; \$500 per kg for $Fe(OH)_3$; and \$75.70 per kg for HTC. The final loadings observed in Figures 21, 24 and 27, which corresponded to final silica concentrations of 30 mg/L were 65 mg/g for $Mg(OH)_2$ at pH 10, 95 mg/g for $Fe(OH)_3$ at pH 10 and 80 mg/g for HTC at pH 12. Hence, $Mg(OH)_2$ can remove 1.74 \$/g, $Fe(OH)_3$ can remove 5.26 \$/g and HTC can remove 0.95 \$/g. In this comparison it does appear that HTC is the most cost effective material for removing silica. However, the pH values were not the same for all materials which plays an important role in silica removal and the chemical costs for the $Mg(OH)_2$ and $Fe(OH)_3$ were obtained for dry chemicals and not for the price of the necessary quantities of $Mg(Cl)_2$, $Fe(Cl)_3$ and NaOH to make freshly precipitated $Mg(OH)_2$ and $Fe(OH)_3$. Therefore, a more comprehensive study of cost could be completed.

Furthermore, work could be completed on the flow through design that could add the chemical doses more efficiently. The current system was designed in such a way that chemical doses had to be entered by hand. While this technique was shown to be effective at removing silica (Experiments 13 through 15), it would be interesting to examine a flow through system with the installation of an inlet to the system containing a slurry of the chemical doses that could be pumped into the system via peristaltic pump. This would provide the opportunity to introduce a variety of doses and more experiments to be completed in a shorter time frame. Therefore, more alternatives could be examined which could provide additional insight. Finally, work could be completed on the flow through system to evaluate the effects of changing HRT on silica removal. This work targeted an HRT that was similar to other work completed so that the investigations could be compared to each other. However, it would be interesting to determine if varying the HRT has an effect on the percent removal of silica.

REFERENCES

1. Al-Mutaz, I. S., & Al-Anezi, I. A. (2002, December). Silica reduction in reverse osmosis desalting plants. In *the 6th Saudi Engineering Conference, King Fahd University of Petroleum and Minerals, Dhahran, Saudi Arabia*.

2. Al-Mutaz, I. S., & Al-Anezi, I. A. (2004). Silica removal during lime softening in water treatment plant. In *International Conference on Water Resources & Arid Environment*. Riyadh: King Saud University.

3. Aljohani, M. S. (2017). Pilot-scale study of the radiation-induced silica removal from underground brackish water in Saudi Arabia. *Radiochimica Acta*, *105*(5), 409-415.

4. Amjad, Z. and Zuhl, R.W. (2011) Factors impacting silica-silicate control agent performance in industrial water systems. *Internation Water Conference*. Orlando, FL.

5. Antony, A., Low, J. H., Gray, S., Childress, A. E., Le-Clech, P., & Leslie, G. (2011). Scale formation and control in high pressure membrane water treatment systems: a review. *Journal of membrane science*, *383*(1-2), 1-16.

6. Baca, Ehren. *Comprehensive Silica Removal with Ferric Compounds for Industrial Wastewater Reuse*. MS Thesis. University of New Mexico. July 2017.

7. Baskaran, T., Christopher, J., & Sakthivel, A. (2015). Progress on layered hydrotalcite (HT) materials as potential support and catalytic materials. *Rsc Advances*, *5*(120), 98853-98875.

8. Batchelor, B., Lasala, M. B., McDevitt, M., & Peacock, E. (1991). Technical and economic feasibility of ultra-high lime treatment of recycled cooling water. *Research Journal of the Water Pollution Control Federation*, 982-990.

9. Belton, D. J., Deschaume, O., & Perry, C. C. (2012). An overview of the fundamentals of the chemistry of silica with relevance to biosilicification and technological advances. *The FEBS journal*, *279*(10), 1710-1720.

10. Benjamin, M. M. (2014). *Water chemistry*. Waveland Press.

11. Bennett, P. C. (1991). Quartz dissolution in organic-rich aqueous systems. *Geochimica et Cosmochimica Acta*, *55*(7), 1781-1797.

12. Bremere, I., Kennedy, M., Mhyio, S., Jaljuli, A., Witkamp, G. J., & Schippers, J. (2000). Prevention of silica scale in membrane systems: removal of monomer and polymer silica. *Desalination*, *132*(1-3), 89-100.

13. Cob, S. S., Hofs, B., Maffezzoni, C., Adamus, J., Siegers, W. G., Cornelissen, E. R., Genceli, F. E., & Witkamp, G. J. (2014). Silica removal to prevent silica scaling in reverse osmosis membranes. *Desalination*, *344*, 137-143.

14. Constantino, V.R.L. and Pinnavaia, T.J. (1995) Basic properties of Mg2+1-xAl3+x layered double hydroxide intercalated by carbonate, hydroxide, chloride and sulphate ions. Inorganic Chemistry, 34, 883-892.

15. Dai, X., Xu, Y., Shen, D., Zhai, X., Dong, B., & Lin, S. (2017). Characterizing and exploring the mechanism of formation of corrosion scales by reusing advanced-softened, silica-rich, oilfield-produced water (ASOW) in a steam-injection boiler. *Journal of Chemical Technology and Biotechnology*, *92*(2), 382-390.

16. Den, W., & Wang, C. J. (2008). Removal of silica from brackish water by electrocoagulation pretreatment to prevent fouling of reverse osmosis membranes. *Separation and Purification Technology*, *59*(3), 318-325.

17. Dudley, L. Y. (2003). Combating the Threat of Silica Fouling in RO Plant-Practical Experiences. *International Desalination and Water Reuse Quarterly*, *12*(4), 28-31.

18. Filmtec, D. (1995). FilmTec Membranes Technical Manual. *The Dow Chemical Company*.

19. Gabelich, C. J., Chen, W. R., Yun, T. I., & Coffey, B. M. (2005). The role of dissolved aluminum in silica chemistry for membrane processes. *Desalination*, *180*(1-3), 307-319.

20. Gill, J. S. (1993). Inhibition of silica—silicate deposit in industrial waters. *Colloids and Surfaces A: Physicochemical and Engineering Aspects*, *74*(1), 101-106.

21. Han, S., Hou, W., Zhang, C., Sun, D., Huang, X., & Wang, G. (1998). Structure and the point of zero charge of magnesium aluminium hydroxide. *Journal of the Chemical Society, Faraday Transactions*, *94*(7), 915-918.

22. Hingston, F. J., & Raupach, M. (1967). The reaction between monosilicic acid and aluminium hydroxide. I. Kinetics of adsorption of silicic acid by aluminium hydroxide. *Soil Research*, *5*(2), 295-309.

23. Howe, K. J., Hand, D. W., Crittenden, J. C., Trussell, R. R., & Tchobanoglous, G. (2012). Principles of water treatment. Hoboken, NJ: John Wiley & Sons.

24. Hunter, R. J. (2001). *Foundations of colloid science*. Oxford university press.

25. Iler, R.K., (1979). The Chemistry of Silica: Solubility, Polymerization, Colloid and Surface Properties and Biochemistry. John Wiley and Sons, New York, USA.

26. Kemmer, F. N., & McCallion, J. (1979). *The NALCO water handbook*. New York: McGraw-Hill.

27. Krivovichev, V. G., & Charykova, M. V. (2014). Number of minerals of various chemical elements: statistics 2012 (a new approach to an old problem). *Geology of Ore Deposits*, *56*(7), 553-559.

28. Latour, I., Miranda, R., & Blanco, A. (2014). Silica removal with sparingly soluble magnesium compounds. Part I. *Separation and Purification Technology*, *138*, 210-218.

29. Masarwa, A., Meyerstein, D., Daltrophe, N., & Kedem, O. (1997). Compact accelerated precipitation softening (CAPS) as pretreatment for membrane desalination II. Lime softening with concomitant removal of silica and heavy metals. *Desalination*, *113*(1), 73-84.

30. McKeague, J. A. (1962). *Silica in Solution in the Presence of Soil and Related Material: Forms, Concentrations and Reactions*. Cornell Univ.

31. Milne, N. A., O'Reilly, T., Sanciolo, P., Ostarcevic, E., Beighton, M., Taylor, K., Mullett, M., Tarquin, A. J., and Gray, S. R. (2014). Chemistry of silica scale mitigation for RO desalination with particular reference to remote operations. *Water research*, *65*, 107-133.

32. Montgomery, J. M. (1985). *Water treatment: principles and design*. John Wiley & Sons.

33. Neofotistou, E., & Demadis, K. D. (2004). Use of antiscalants for mitigation of silica (SiO2) fouling and deposition: fundamentals and applications in desalination systems. *Desalination*, *167*, 257-272.

34. Ning, R. Y. (2005). Silica in Natural Waters. *Water Encyclopedia*, *4*, 548-551.

35. Ning, R. Y. (2010). Reactive silica in natural waters—A review. *Desalination and water treatment*, *21*(1-3), 79-86.

36. Peslier, A. H., Woodland, A. B., Bell, D. R., Lazarov, M., and Lapen, T. J. (2012), Metasomatic control of water contents in the Kaapvaal cratonic mantle, *Geochim. Cosmochim. Acta*, 97, 213–246.

37. Roalson, S. R., Kweon, J., Lawler, D. F., & SPEITEL, G. E. (2003). Enhanced softening: effects of lime dose and chemical additions. *Journal (American Water Works Association)*, *95*(11), 97-109.

38. Rocha, J., Del Arco, M., Rives, V., & Ulibarri, M. A. (1999). Reconstruction of layered double hydroxides from calcined precursors: a powder XRD and 27 Al MAS NMR study. *Journal of Materials Chemistry*, *9*(10), 2499-2503.

39. Sanks, R. L. (1982). Water treatment plant design: for the practicing engineer. In *Water treatment plant design: for the practicing engineer*. Ann Arbor Sci.

40. Sasan, K., Brady, P. V., Krumhansl, J. L., & Nenoff, T. M. (2017). Removal of dissolved silica from industrial waters using inorganic ion exchangers. *Journal of water process engineering*, *17*, 117-123.

41. Schott, H. (1981). Electrokinetic studies of magnesium hydroxide. *Journal of pharmaceutical sciences*, *70*(5), 486-489.

42. Schutz, A., & Biloen, P. (1987). Interlamellar chemistry of hydrotalcites: I. Polymerization of silicate anions. *Journal of Solid State Chemistry*, *68*(2), 360-368.

43. Sheikholeslami, R., & Bright, J. (2002). Silica and metals removal by pretreatment to prevent fouling of reverse osmosis membranes. *Desalination*, *143*(3), 255-267.

44. Sheikholeslami, R., & Tan, S. (1999). Effects of water quality on silica fouling of desalination plants. *Desalination*, *126*(1-3), 267-280.

45. Sheikholeslami, R., Al-Mutaz, I. S., Koo, T., & Young, A. (2001). Pretreatment and the effect of cations and anions on prevention of silica fouling. *Desalination*, *139*(1-3), 83-95.

46. Sims, Magdalena. *Examination of Silica Removal with Solids Recycle for Reverse Osmosis Pretreatment*. MS Thesis. University of New Mexico. July, 2015.

47. Stumm, W., & Morgan, J. J. (1996). Aquatic Chemistry, John Wiley & Sons. *Inc., New York*.

48. Taylor, P. (1995). Interactions of silica with iron oxides: effects on oxide transformations and sorption properties (No. AECL--11257). Atomic Energy of Canada Ltd.

49. Tokoro, C., Suzuki, S., Haraguchi, D., & Izawa, S. (2014). Silicate removal in aluminum hydroxide co-precipitation process. *Materials*, *7*(2), 1084-1096.

50. Wang, Y., Wang, G., Wang, H., Liang, C., Cai, W., & Zhang, L. (2010). Chemical-template synthesis of micro/nanoscale magnesium silicate hollow

spheres for waste-water treatment. *Chemistry-A European Journal*, *16*(11), 3497-3503.

51. White, A. F. (2003). Natural weathering rates of silicate minerals. *Treatise on geochemistry*, *5*, 605.

52. White, D. E., Brannock, W. W., & Murata, K. J. (1956). Silica in hot-spring waters. *Geochimica et Cosmochimica Acta*, *10*(1-2), 27-59.

53. Yokoyama, T., Nakazato, T., & Tarutani, T. (1980). Polymerization of silicic acid adsorbed on iron (III) hydroxide. *Bulletin of the Chemical Society of Japan*, *53*(4), 850-853.

54. Zhong, W., Li, H., Ye, Y., & Chen, V. (2016). Evaluation of silica fouling for coal seam gas produced water in a submerged vacuum membrane distillation system. *Desalination*, *393*, 52-64.

55. Zhu, J., Tang, C., Wei, J., Li, Z., Laipan, M., He, H., Liang, X., Tao, Q., and Cai, L. (2018). Structural effects on dissolution of silica polymorphs in various solutions. *Inorganica Chimica Acta*, *471*, 57-65.